

# Making Quantum Bits

C. M. Marcus  
Harvard University

## Collaborators:

Jason Petta  
Alex Johnson  
Edward Laird  
Prof. Amir Yacoby (Weizmann)

Jacob Taylor  
Hans-Andreas Engel  
Prof. Mikhail Lukin

## Material:

M. Hanson, A. C. Gossard (UCSB)

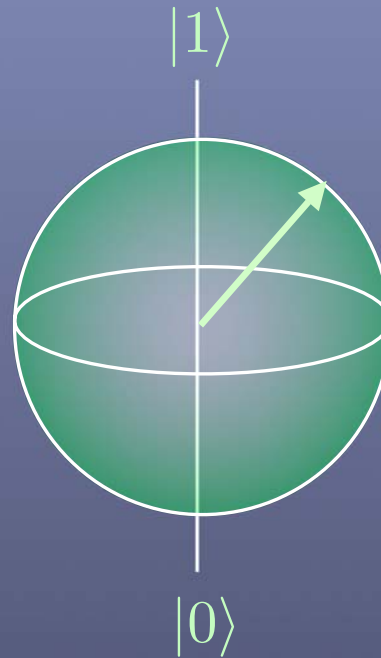
## Support:

DARPA, ARO/ARDA, NSF

## Classical Bit

$[0, 1]$

## Quantum Bit



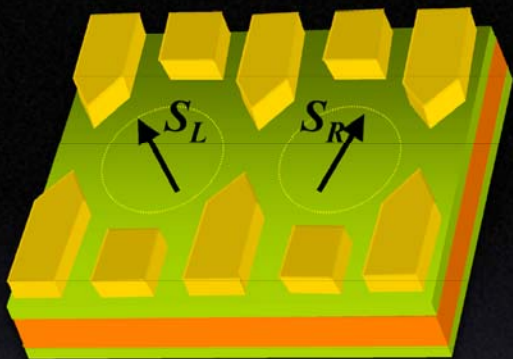
$$\alpha|0\rangle + \beta|1\rangle$$

## Outline:

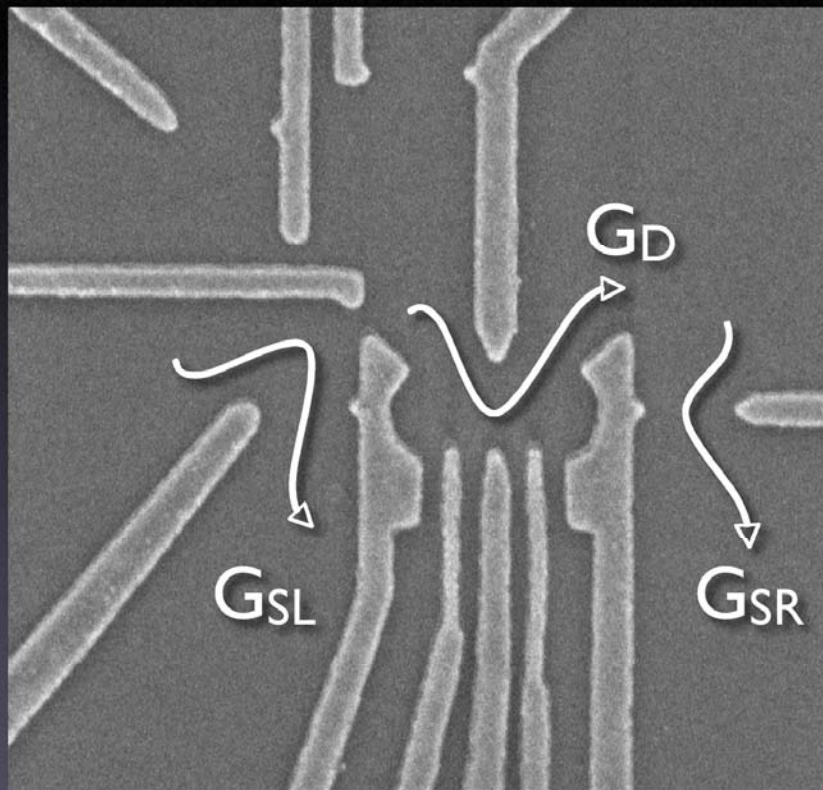
- Control and read-out with Few Electrons
- Measuring Spin Relaxation Time
- Fast Control of Exchange Interaction
- Swap Operation and Rabi Oscillations of Spin States
- Spin Echo, Measurement of T2

— quantum control —  
↓

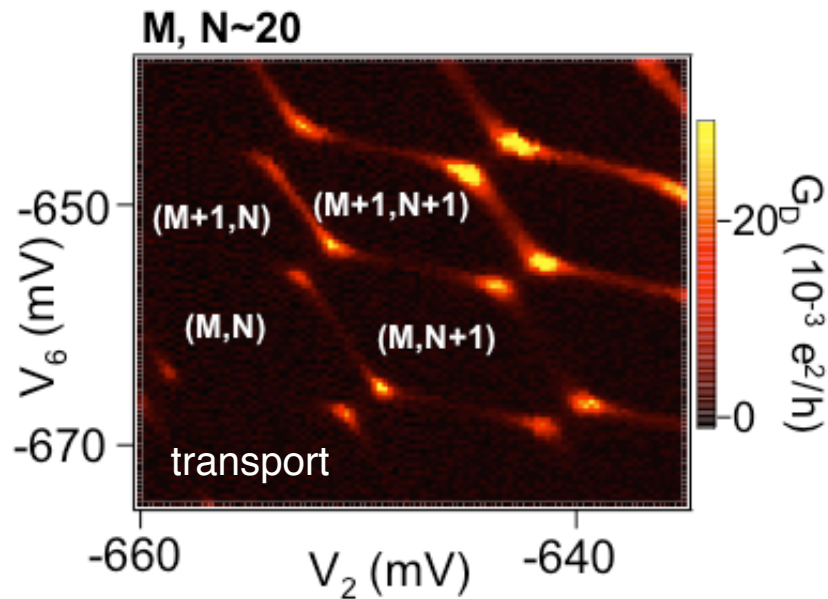
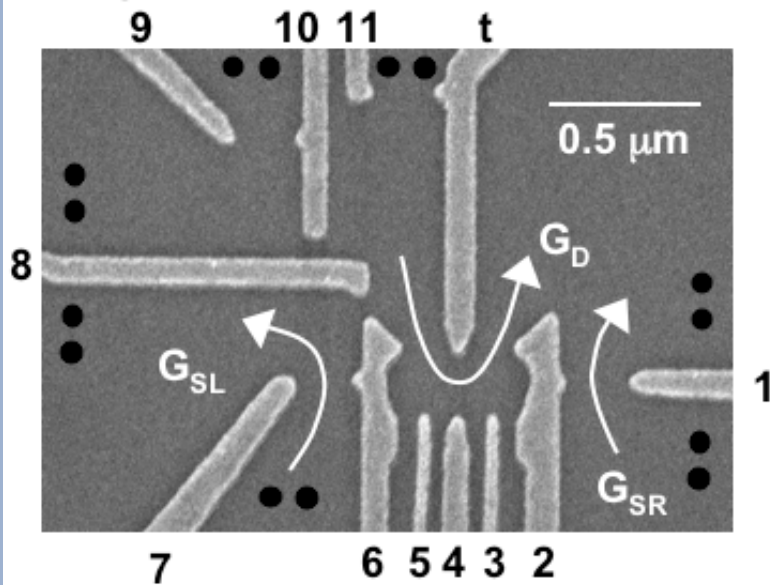
# Semiconductor Doublet Dot Device



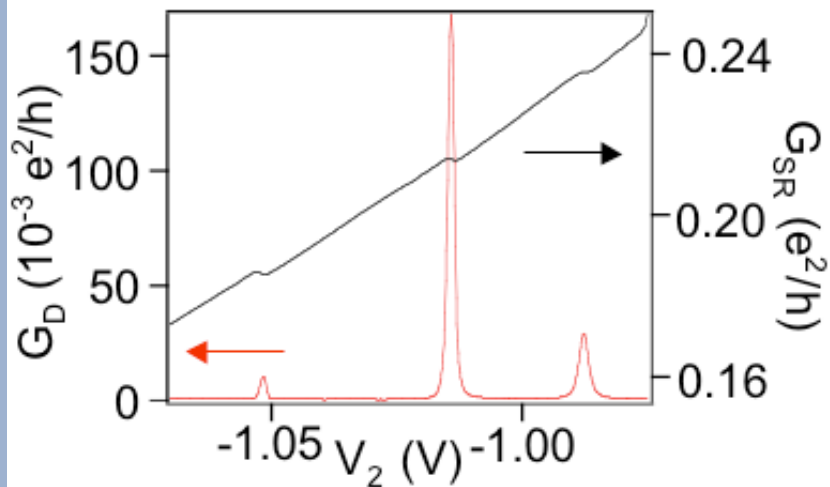
2D  
electron gas



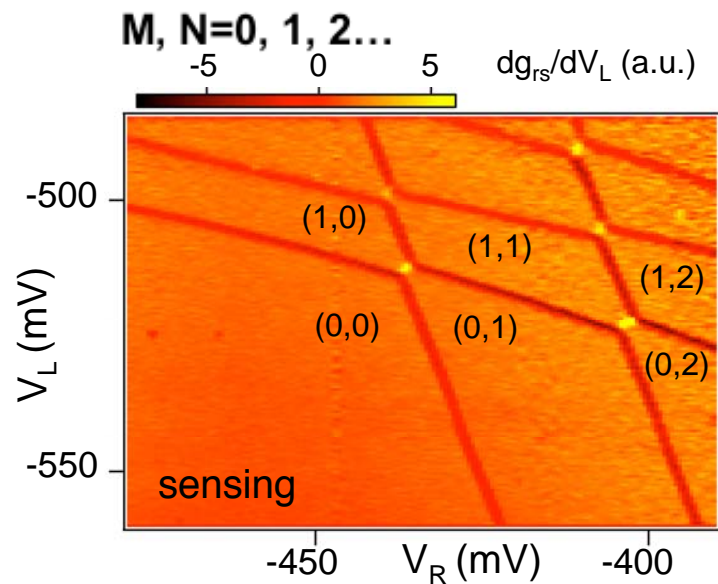
## Charge transport in a double dot



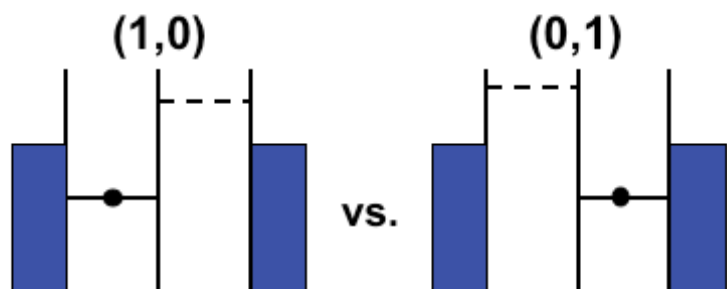
## Charge sensing



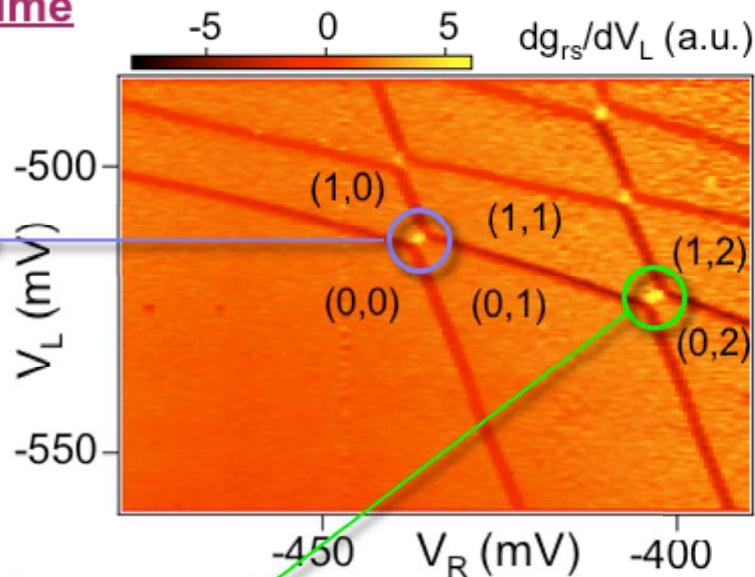
QPC sensing: Field *et al.*, PRL **70**, 1311 (1993)



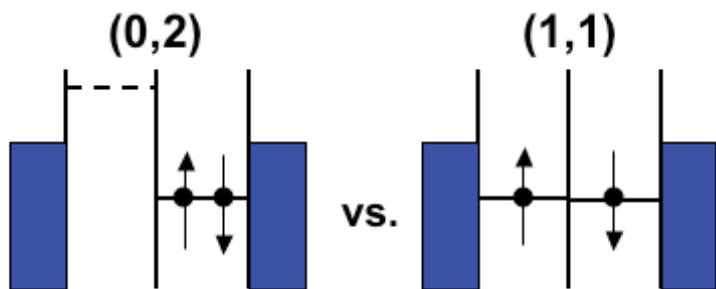
## Charge physics: The one electron regime



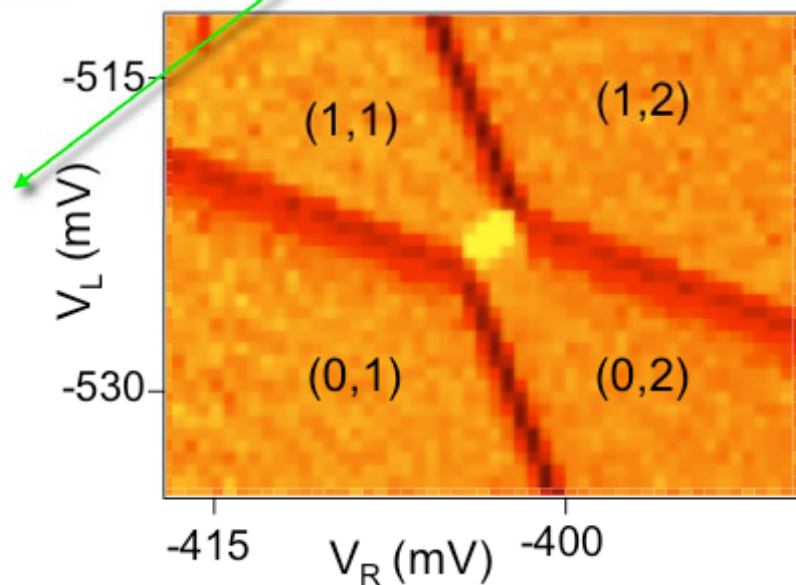
$T_1 \sim 15$  ns,  $T_2 \sim 1$  ns  
(Fujisawa, Hayashi, Petta)



## Spin physics: The two electron regime

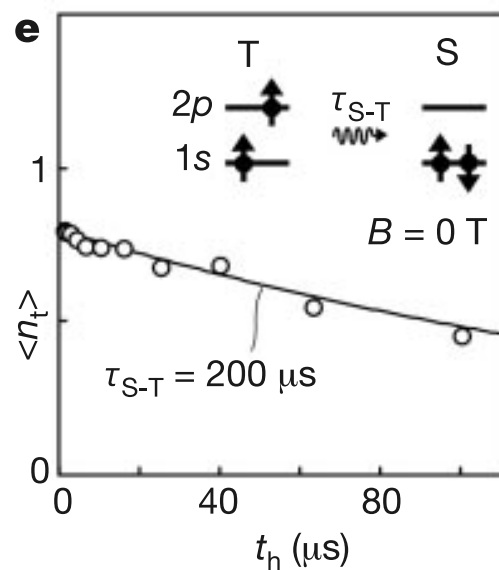
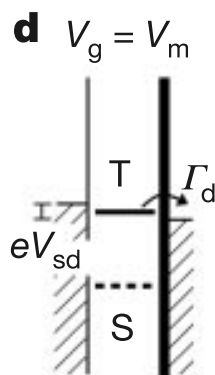
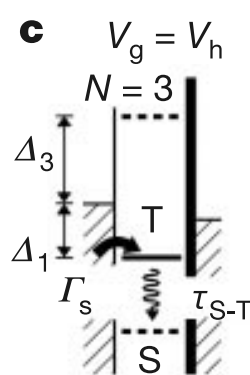
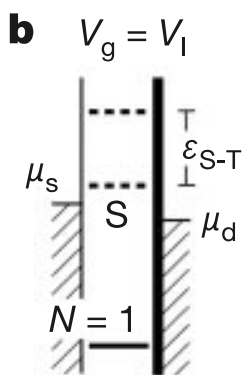
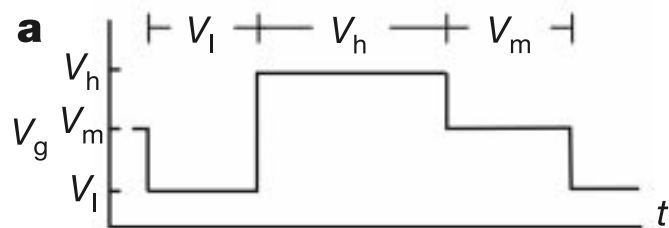


$T_1 \sim 1$  ms,  $T_2 = ?$        $T_1 = ?$ ,  $T_2 = ?$   
(Fujisawa, Elzerman, Kroutvar)



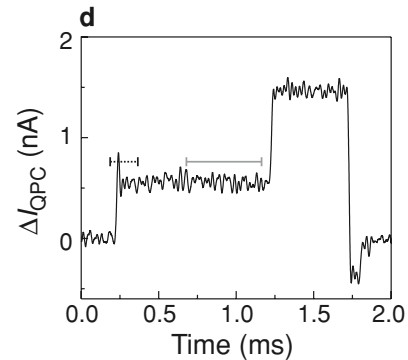
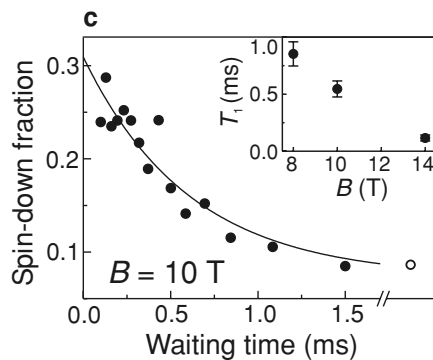
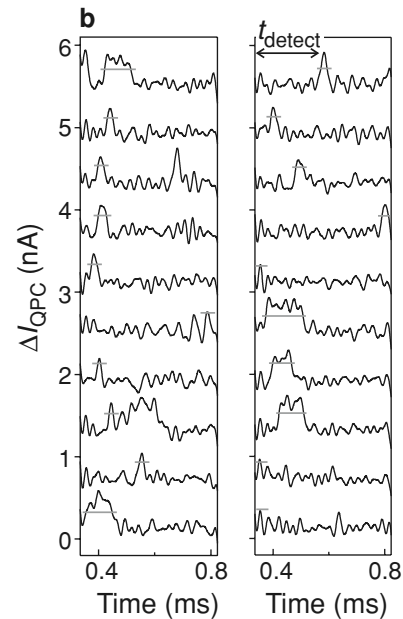
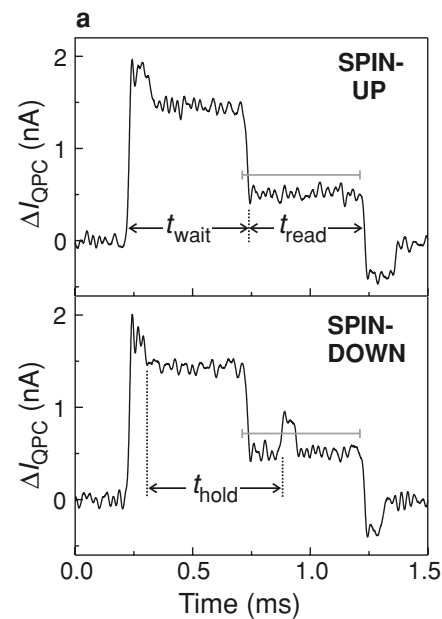
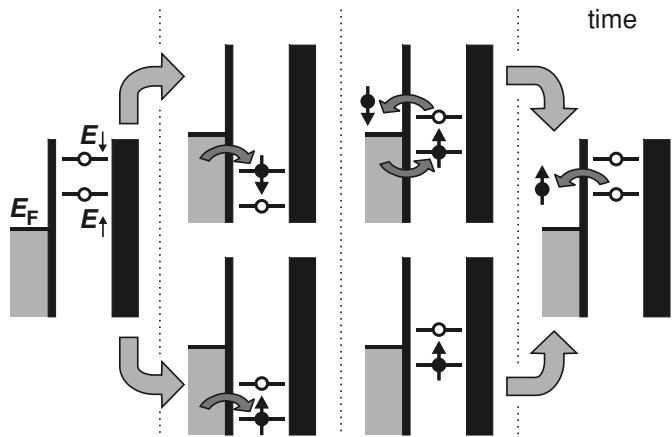
**Allowed and forbidden transitions in artificial hydrogen and helium atoms**

Toshimasa Fujisawa\*, David Guy Austing\*†, Yasuhiro Tokura\*,  
Yoshiro Hirayama\*‡ & Seigo Tarucha\*§||



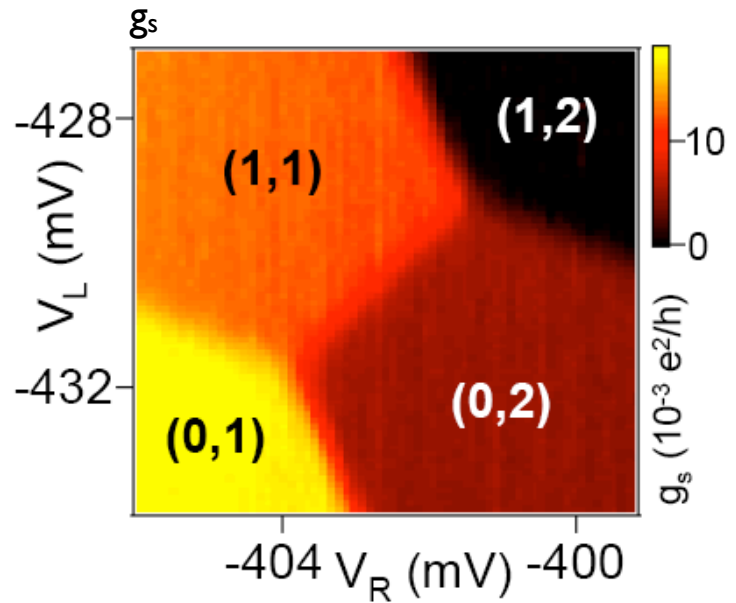
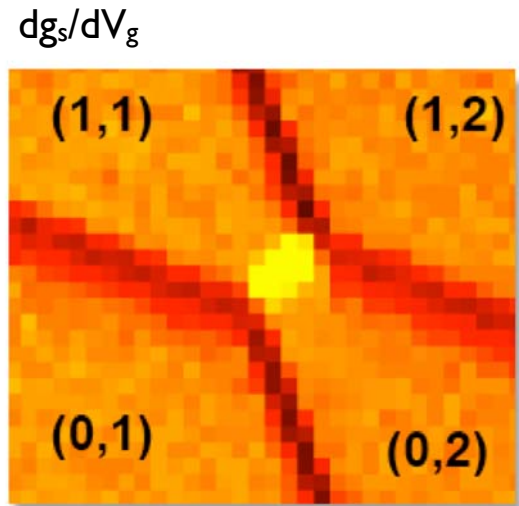
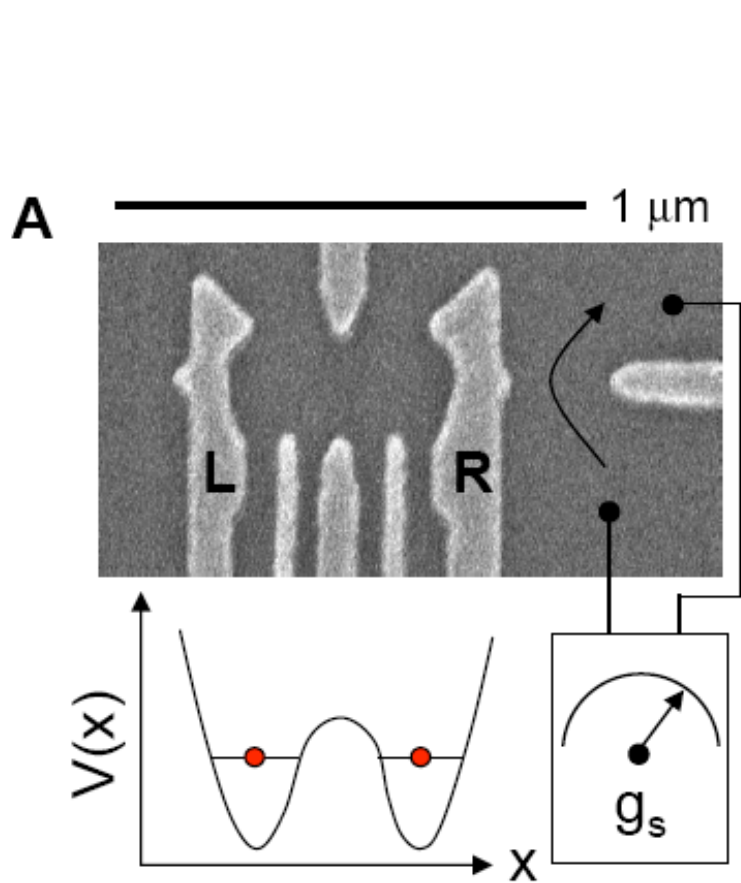
# Single Shot Readout Gives Similar T1 times for Zeeman Split Spin Levels

Delft Group



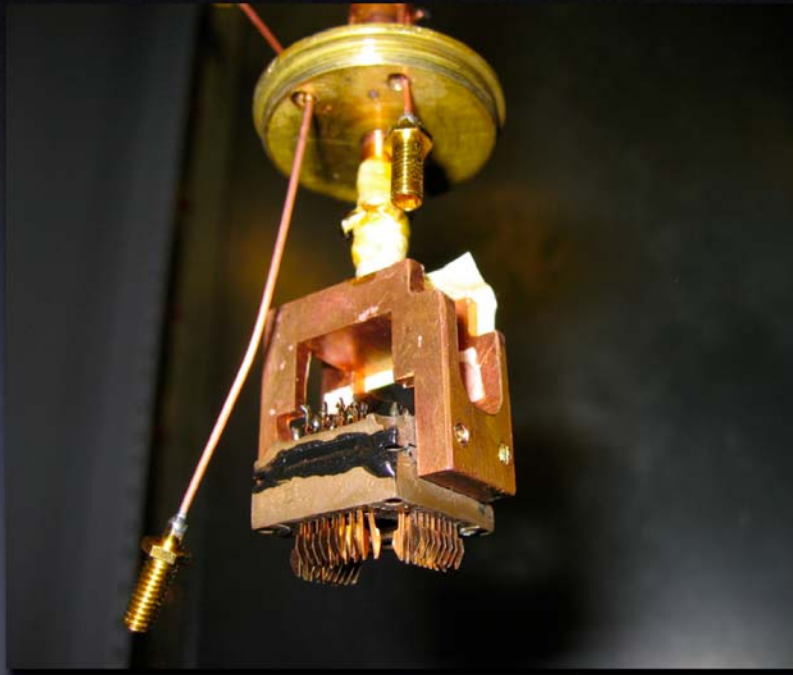
R. Hanson, B. Witkamp, L.M.K. Vandersypen, L.H. Willem van Beveren, J.M. Elzerman, and L.P. Kouwenhoven, Phys. Rev. Lett. **91**, 196802 (2003).

# Spin Relaxation and Dephasing: The Two-Electron System

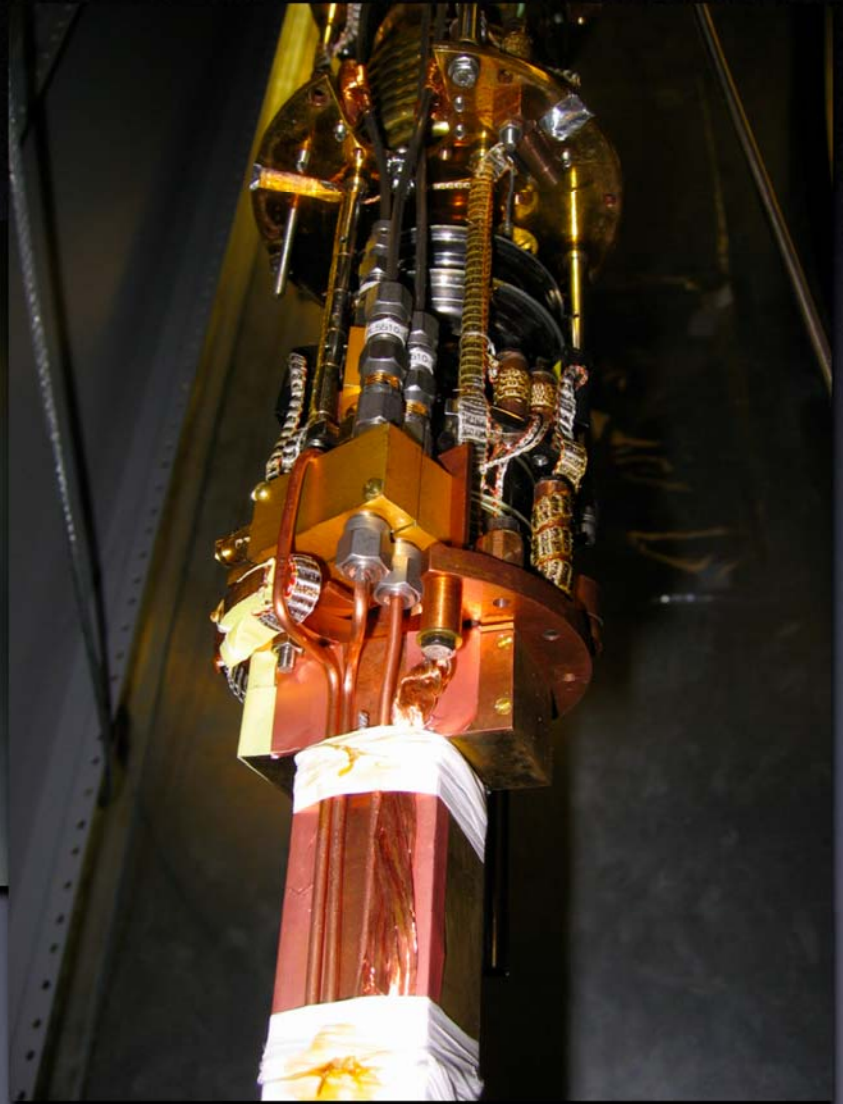


J. R. Petta, A. C. Johnson, J. Taylor, A. Yacoby,  
M.D. Lukin, CMM (2005)

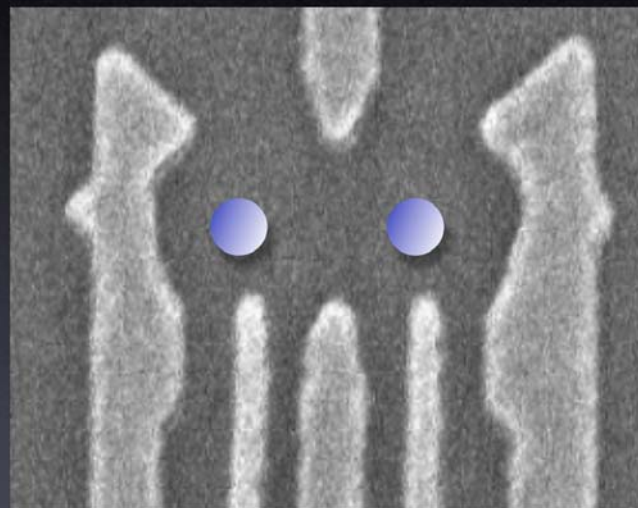
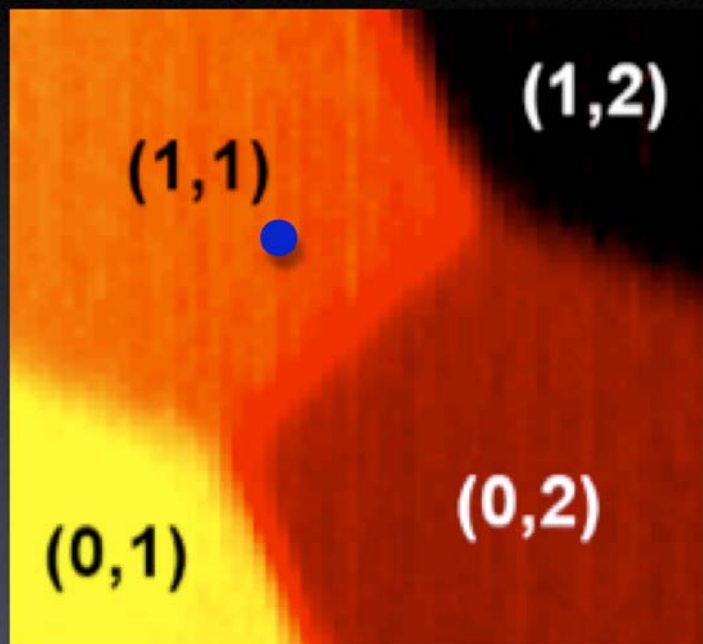
# High-bandwidth dilution refrigerator



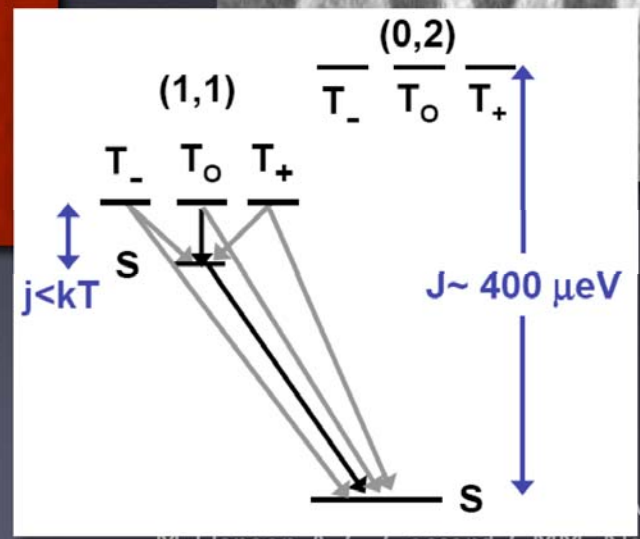
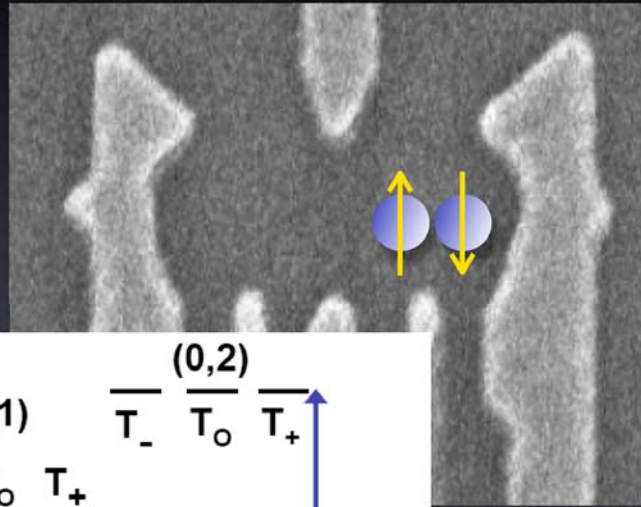
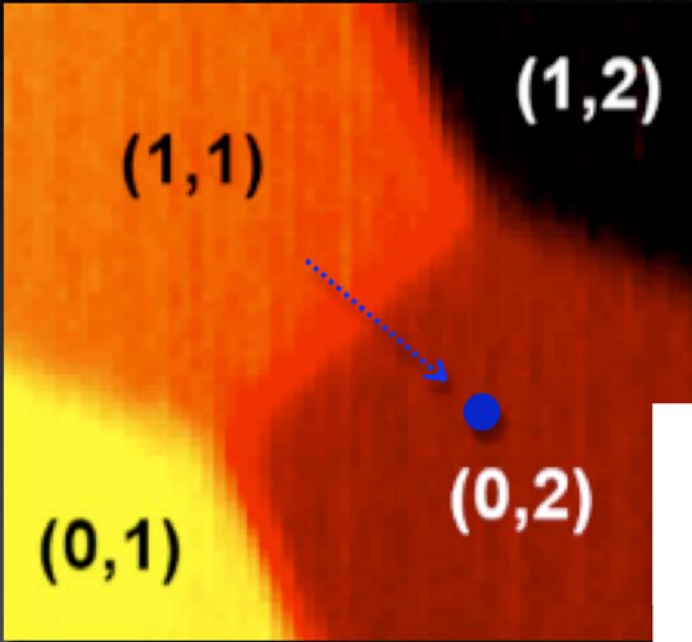
Pulses with 1 ns rise time applied  
using Tektronix AWG 520  
arbitrary waveform generators



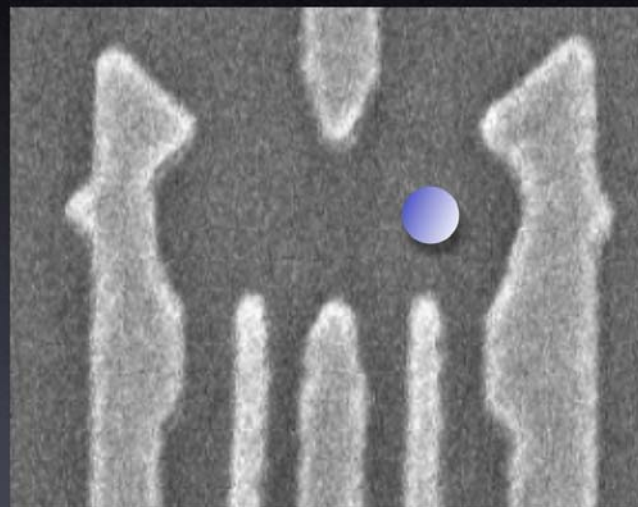
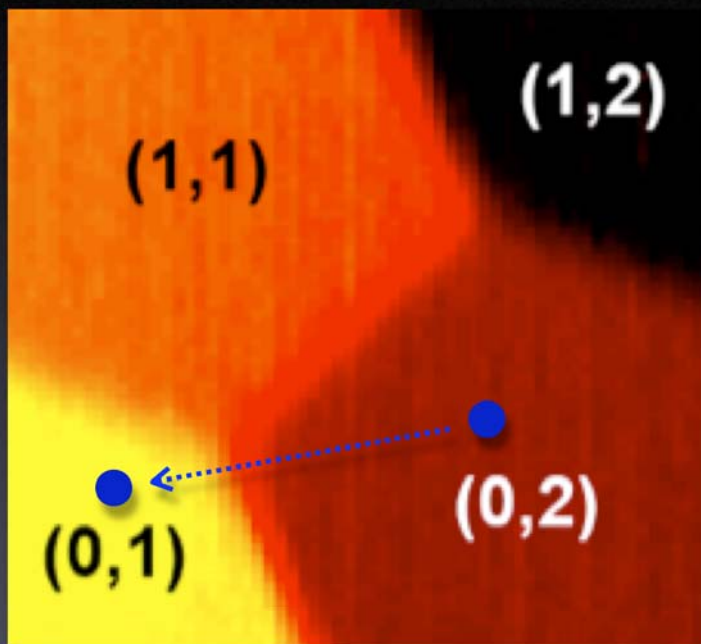
# Pulsed-Gate Measurement of Spin Relaxation



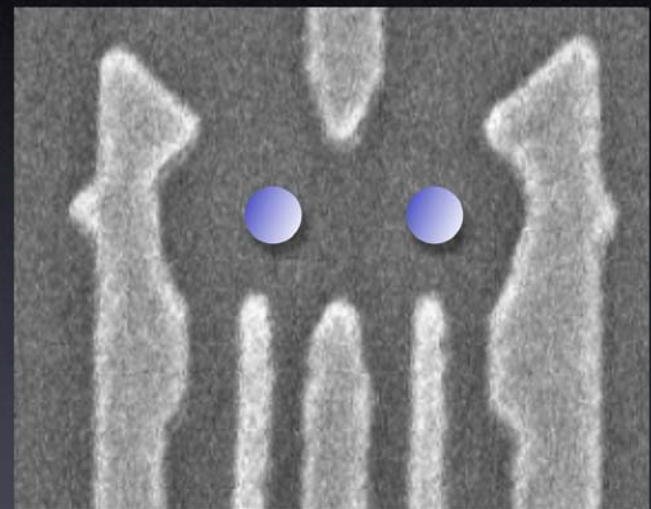
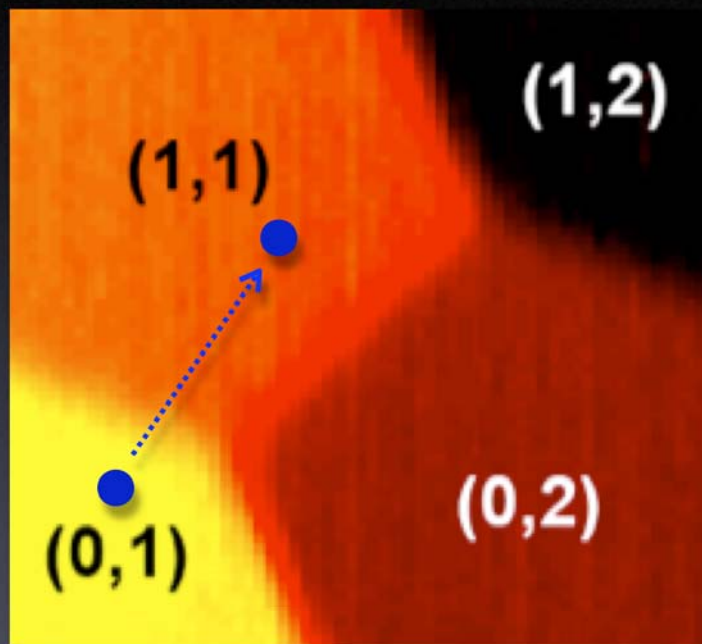
# Pulsed-Gate Measurement of Spin Relaxation



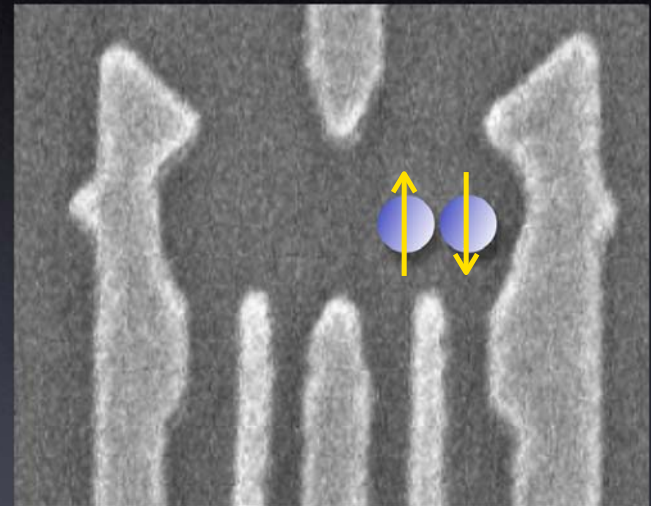
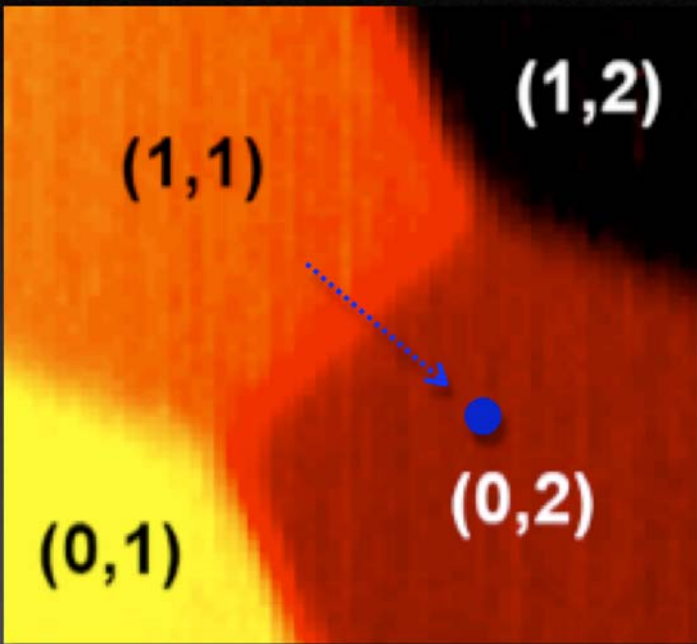
# Pulsed-Gate Measurement of Spin Relaxation



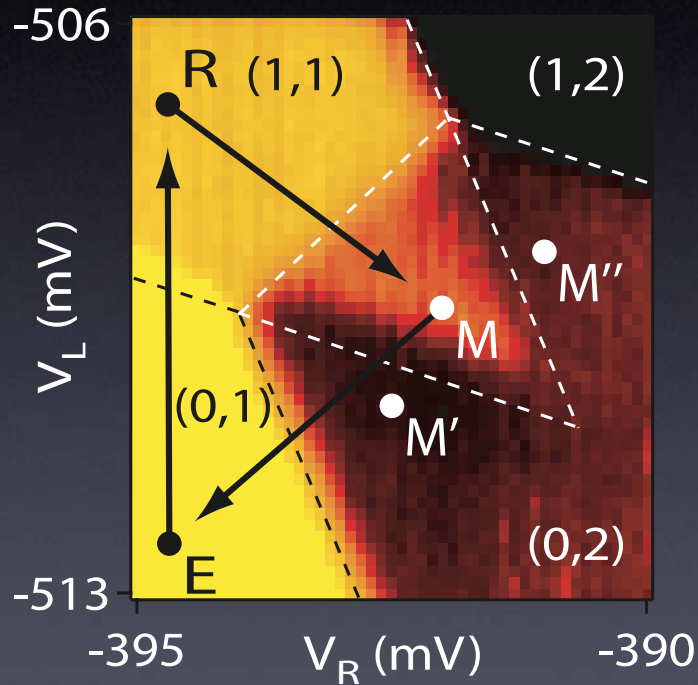
# Pulsed-Gate Measurement of Spin Relaxation



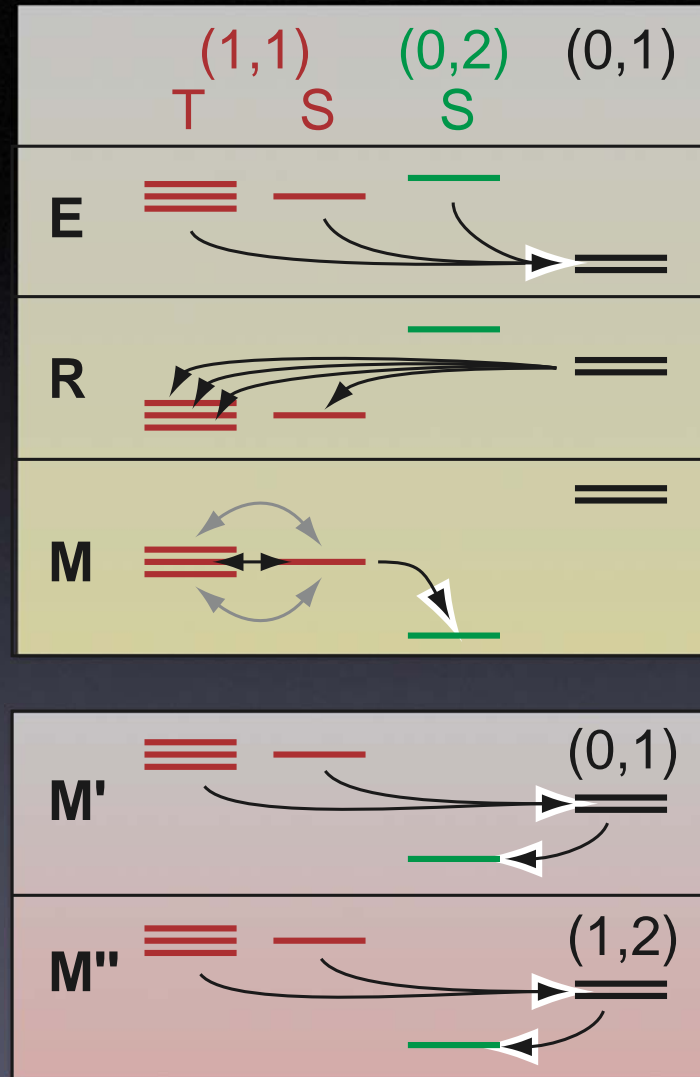
# Pulsed-Gate Measurement of Spin Relaxation



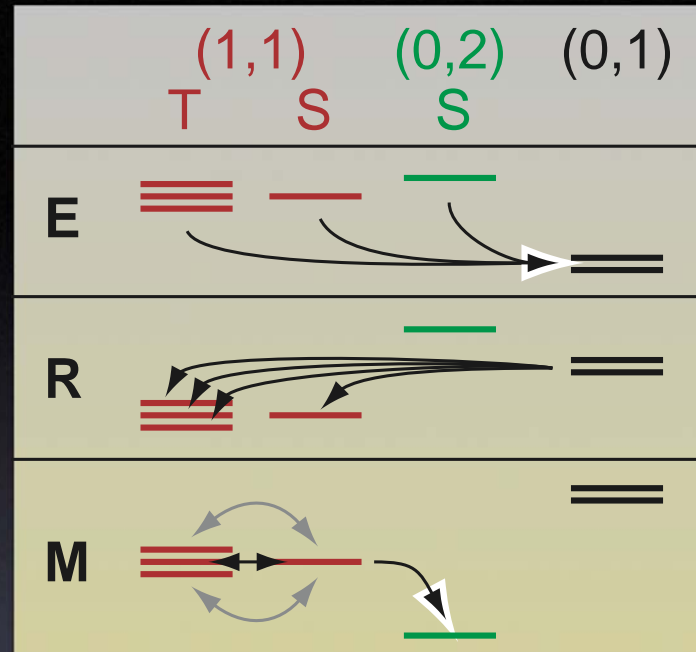
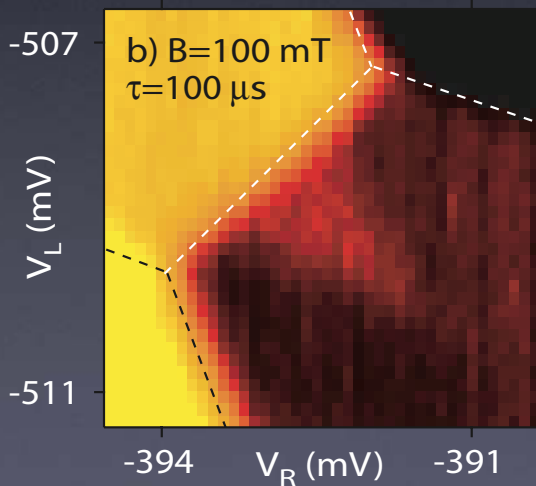
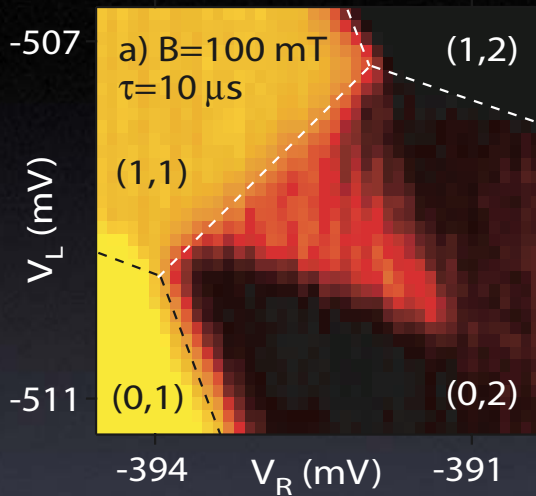
# Spin relaxation: Getting Stuck in (1,1)



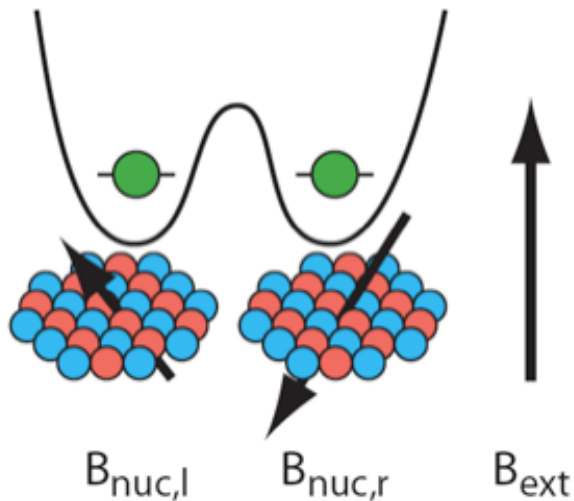
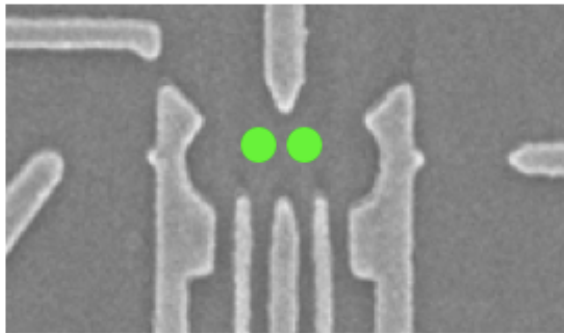
In "measurement triangle"  
dark: transition to  $(0,2)$  occurs  
light: transition to  $(0,2)$  blocked



# Spin relaxation: Getting Stuck in (1,1)



## Effective nuclear field from Hyperfine interaction



Large ensemble with random spin orientations, slow internal dynamics...

Quasistatic effective field

$$\mathbf{B}_{nuc} = b_0 \sum_k |\psi(r_k)|^2 \mathbf{I}_k$$

$$rms\ B_{nuc} = b_0 \sqrt{I_0(I_0 + 1)/N}$$

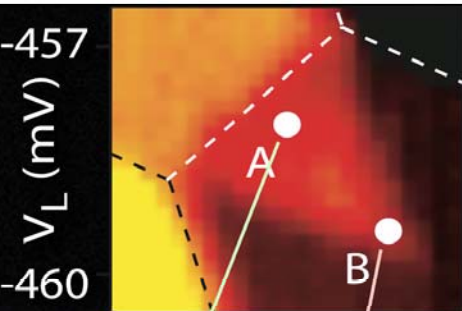
$$\text{GaAs: } b_0 = 3.47\ \text{T},\ I_0 = 3/2$$

$$\text{Our device: } N \sim 10^6 - 10^7$$

$$B_{nuc} \sim 2-6\ \text{mT},\ t_{nuc} \sim 3-10\ \text{ns}$$

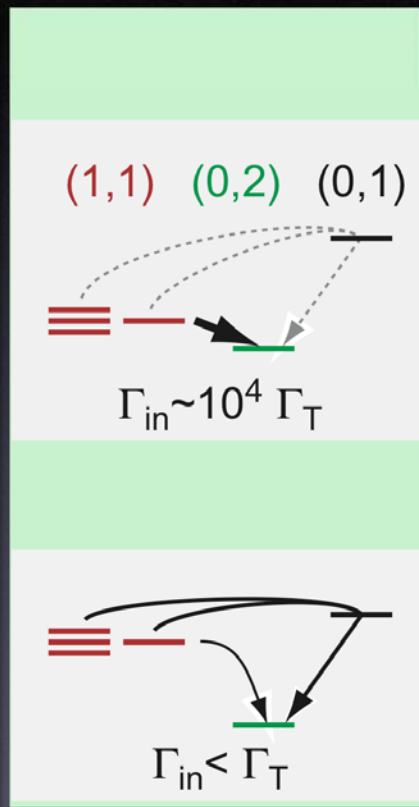
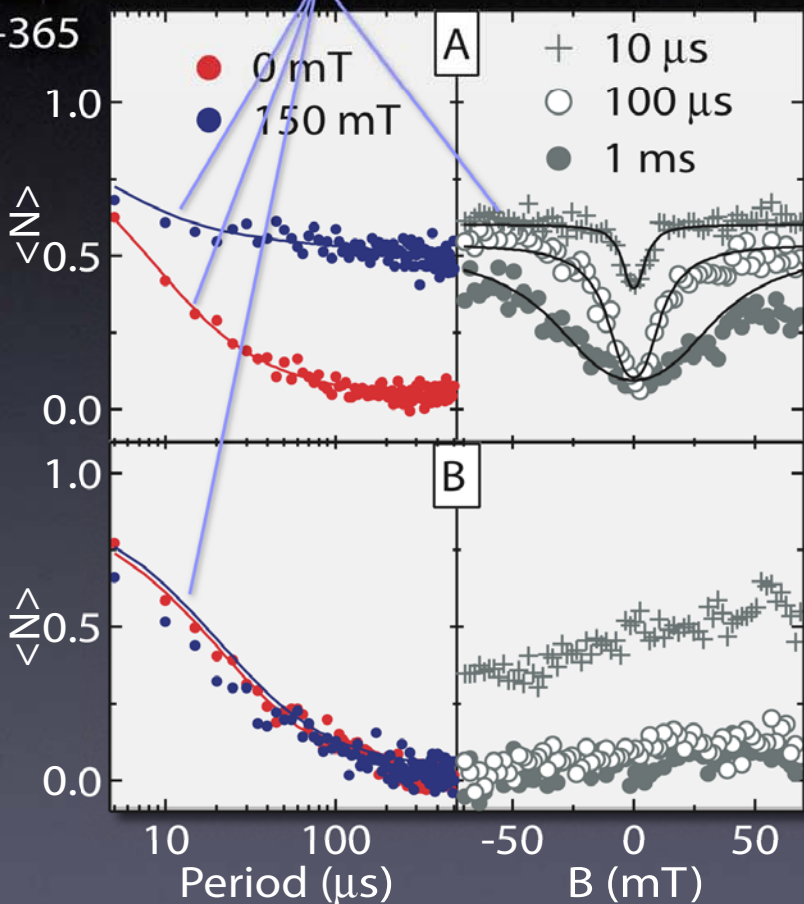
# Field dependence of relaxation from (1,1) to (0,2)s.

theory (inelastic-hyperfine & thermal)

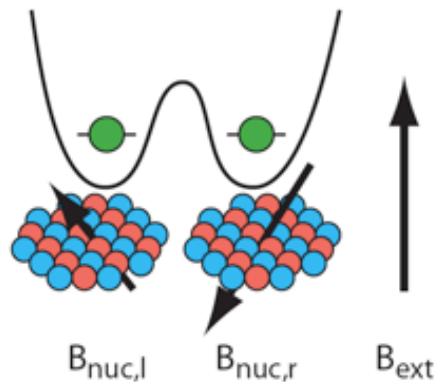


Dominated by  
Hyperfine  
Interaction

Dominated by  
Thermal  
Activation



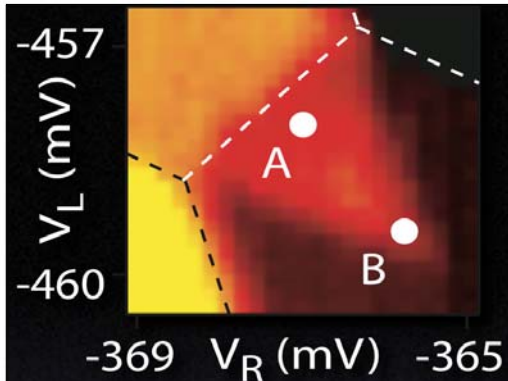
## Nuclear fields - Effect on interdot tunneling



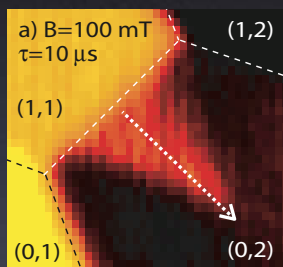
$$B_{nuc} \sim 2-6 \text{ mT}, t_{nuc} \sim 3-10 \text{ ns}$$

	$B_{ext} = 0$	$B_{ext} \gg B_{nuc}$
Spin mixing	All spin states mix in time $t_{nuc}$	$S \leftrightarrow T_0$ : full mixing in $t_{nuc}$ $S \leftrightarrow T_{\pm}$ : fractional mixing $(B_{nuc}/B_{ext})^2$ in $t_{nuc}$
Interdot tunneling (assume $\Gamma_{in}^{-1} \gg t_{nuc}$ )	Uniform tunnel rate $\Gamma_{in}/4$	50% tunnel with rate $\Gamma_{in}/2$ 50% tunnel with rate $(B_{nuc}/B_{ext})^2 \Gamma_{in}/2$
Thermally activated tunneling to the leads	spin-independent: uniform rate $\Gamma_T$ at all fields	

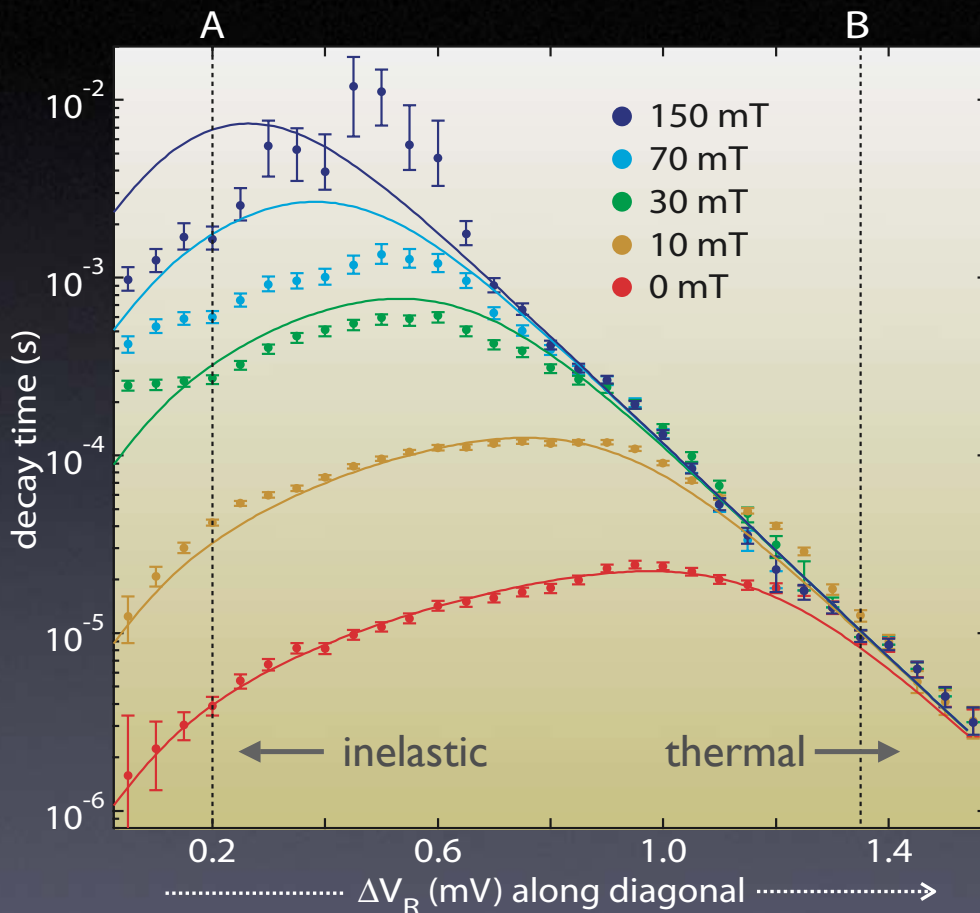
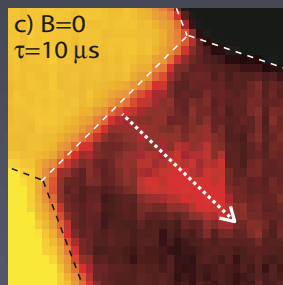
# Field dependence of relaxation from (1,1) to (0,2)s.



B=100 mT



B=0 mT



## Influence of nuclear spin on chemical reactions: Magnetic isotope and magnetic field effects (A Review)

(spin dynamics/photochemistry/radical pairs/isotope enrichment)

NICHOLAS J. TURRO

Department of Chemistry, Columbia University, New York, New York 10027

Contributed by Nicholas J. Turro, November 1, 1982

**ABSTRACT** The course of radical pairs may depend on the nuclear spins in the pairs. The influence of nuclear spin on the reaction when the radical pairs are formed is that allows a certain degree of rotational motion of the partners. Under the proper conditions, the nuclear spin crossing between triplet and singlet states is shown that this dependence of reaction rate on nuclear spin leads to a magnetic isotope effect which provides a means of separating nuclear spins rather than nuclear magnetic field effect on the chemistry of radical pairs. A means of influencing the course of weak magnetic field effects on the chemistry of radical pairs.

### PHYSICAL MODEL

"Spin" is the term used to describe a property associated with a particle. A physical model of spin is based on the supposition that this property arises from a body rotating about an axis. A model allows recognition of the effects of quantum mechanical

clear spins to operate on the odd electrons. Under the proper conditions, the nuclear spin crossing between triplet and singlet states is shown that this dependence of interaction rate on nuclear spin leads to a magnetic isotope effect which provides a means of separating nuclear spins rather than nuclear magnetic field effect on the chemistry of radical pairs which provides a means of influencing the course of polymerization by the application of weak magnetic fields.

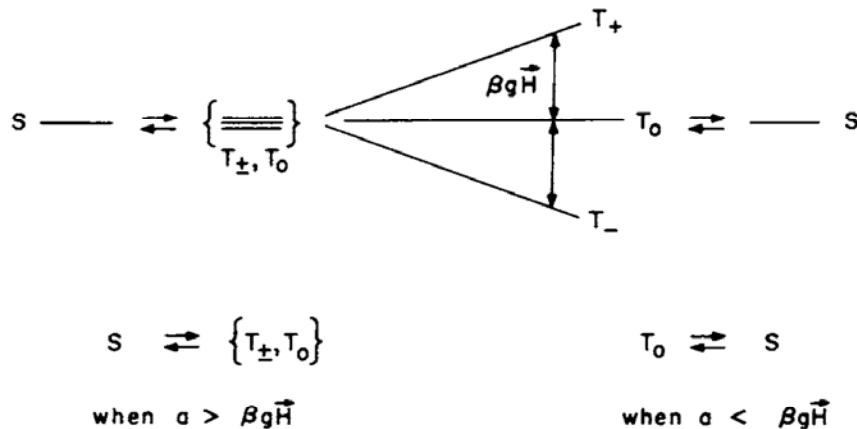
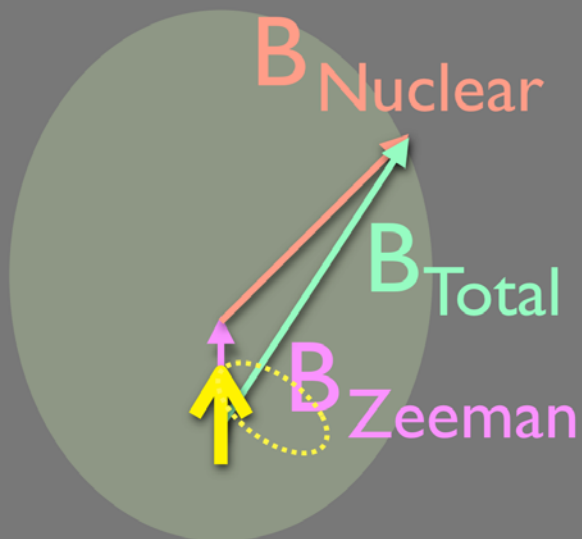
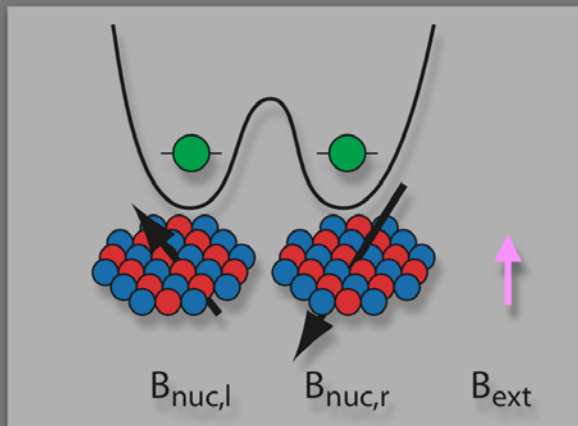


FIG. 16. Schematic representation of the Zeeman interaction  $\beta g \vec{H}$  on the energetic separation of  $T_+$ ,  $T_-$ , and  $T_0$ . When the Zeeman interaction is small relative to other interactions (such as the hyperfine interaction whose strength is given by  $a$ , the hyperfine splitting constant), the triplet and singlet states are energetically degenerate, and all three triplet sublevels interconvert with the singlet state. When  $\beta g \vec{H}$  is large relative to  $a$ , only  $T_0 \rightarrow S$  ISC occurs. The effect of  $\beta g \vec{H}$  is to split  $T_+$  and  $T_-$  from S energetically and thereby inhibit ISC from or to these sublevels.

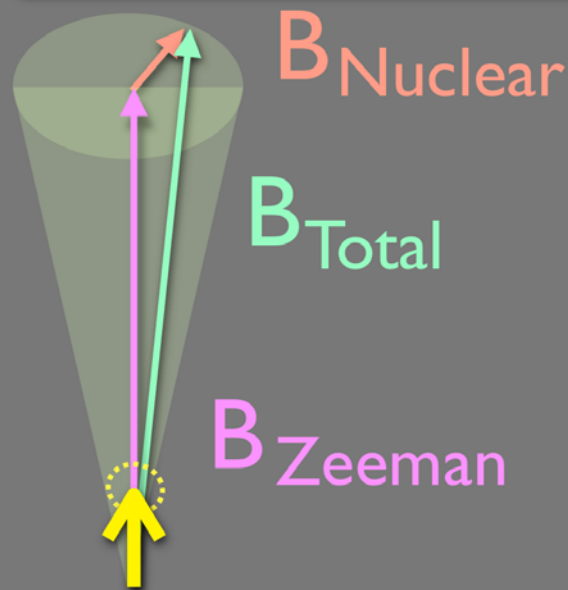
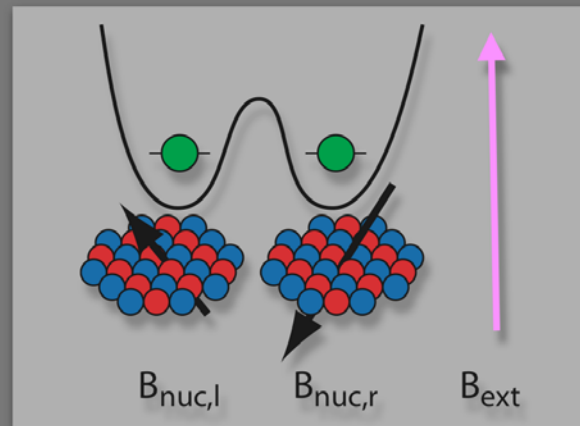
applied along the z axis,  $\alpha$  or  $\beta$  position (Fig. 16) about the z axis with radical pairs; DBK, dibutylammonium chloride;

$$B_{\text{Zeeman}} \sim B_{\text{Nuclear}}$$



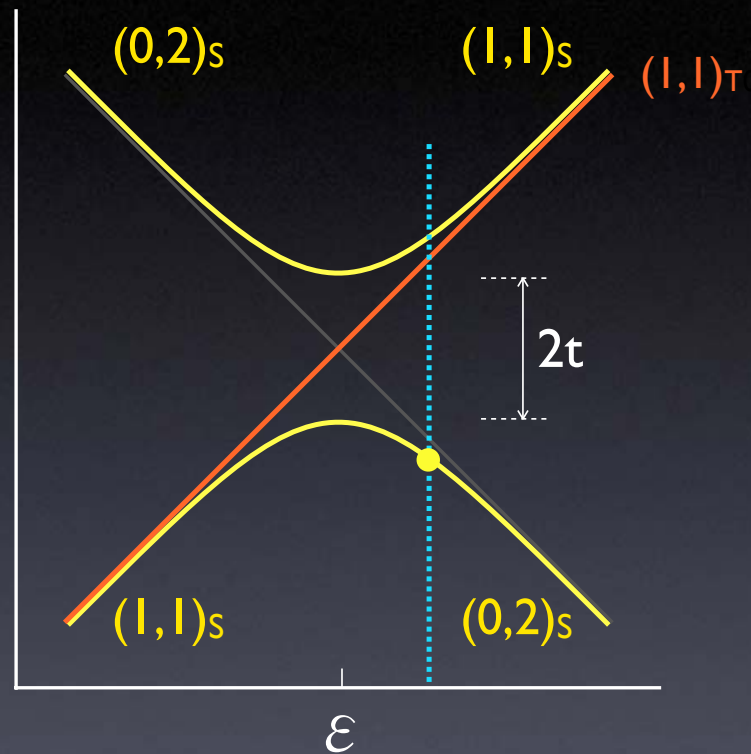
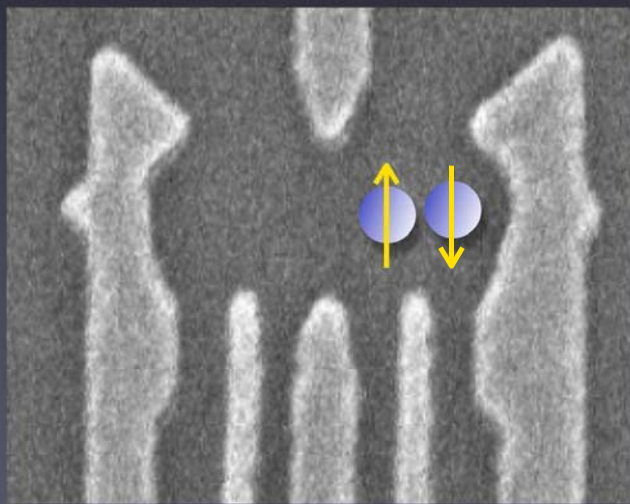
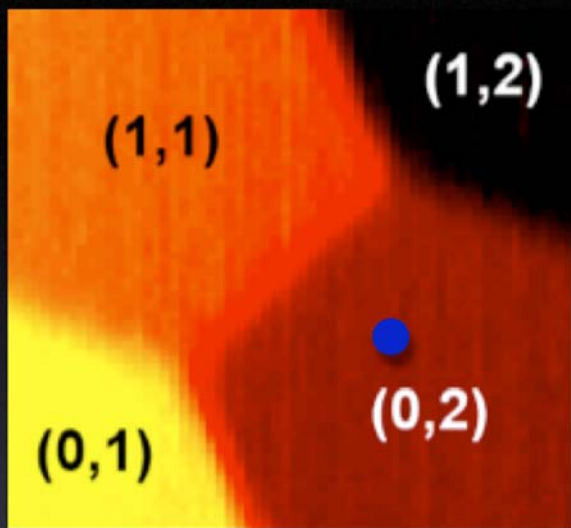
T1, T2 short

$$B_{\text{Zeeman}} \gg B_{\text{Nuclear}}$$



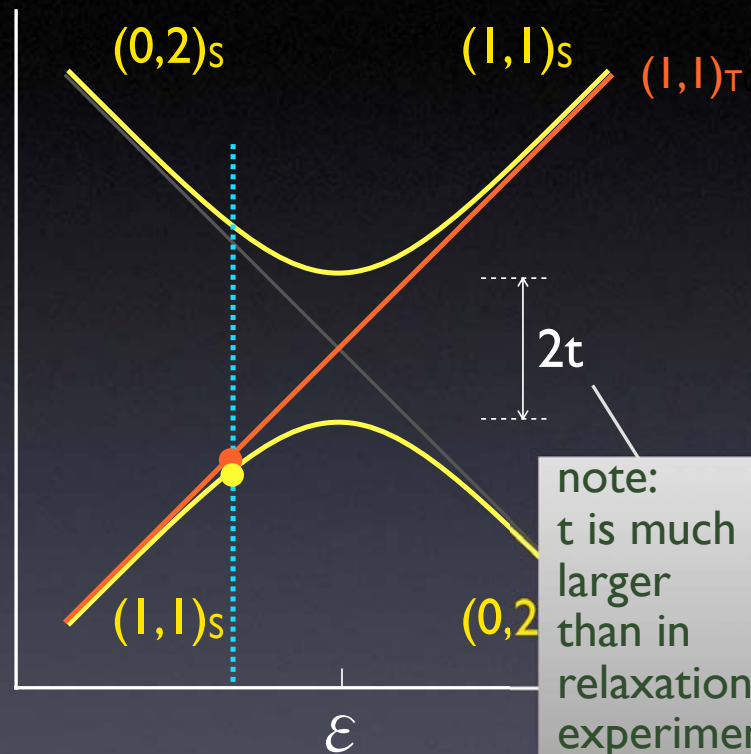
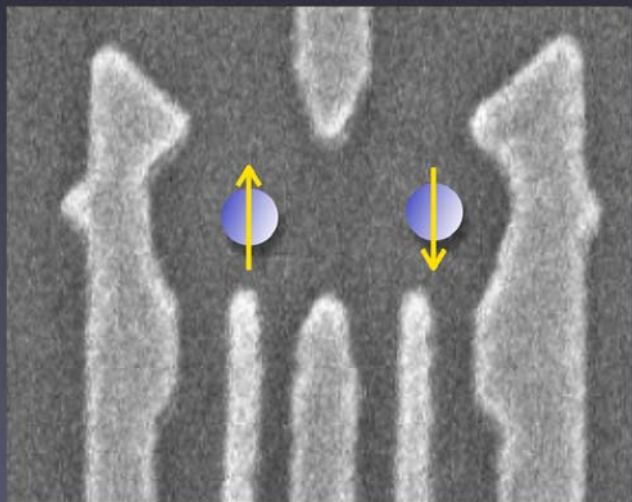
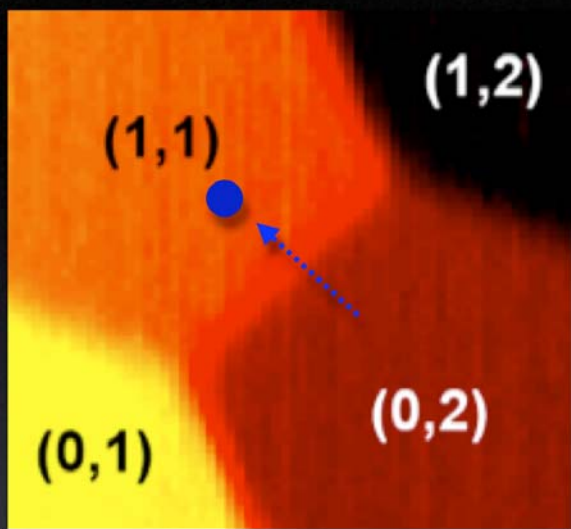
T1 long; T2 short

# Measuring Spin Dephasing ( $T_2^*$ ): Time-domain Interferometry



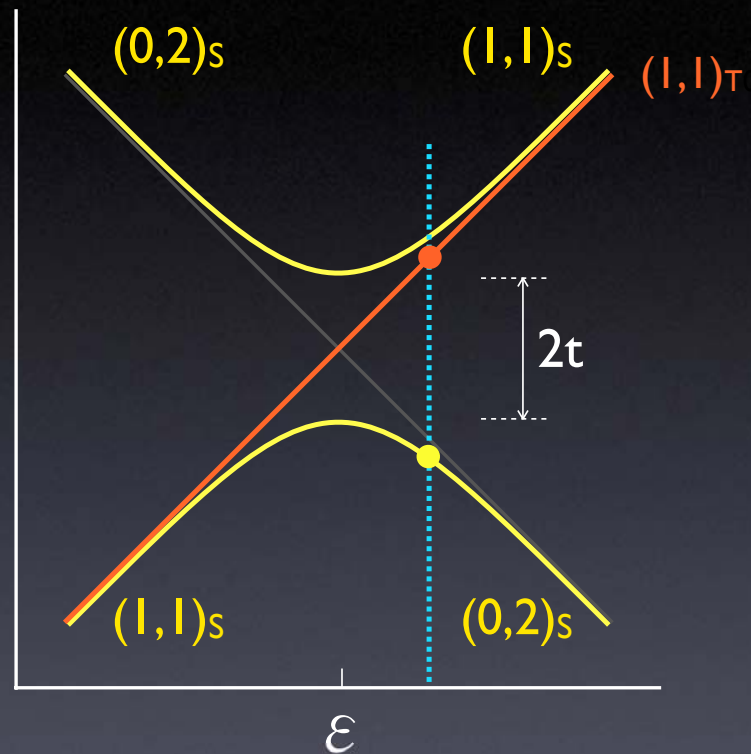
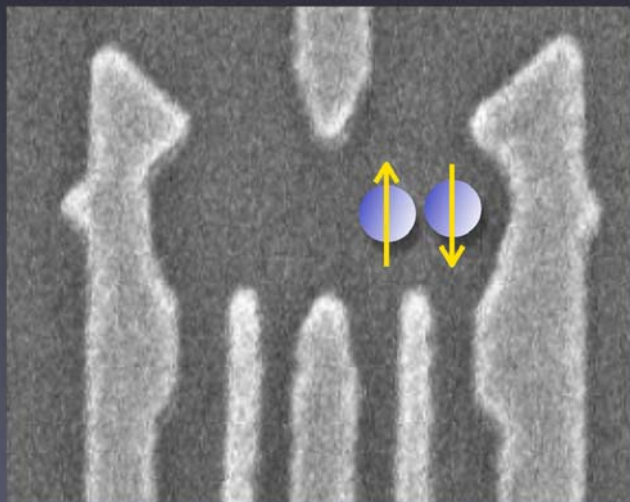
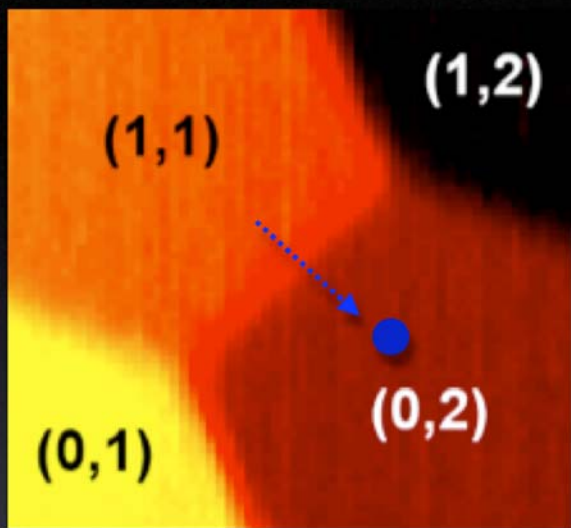
J. R. Petta, A. C. Johnson, J. Taylor, A. Yacoby, M.D. Lukin, M. Hanson, A. C. Gossard, CMM Science (in press) (2005)

# Measuring Spin Dephasing ( $T_2^*$ ): Time-domain Interferometry

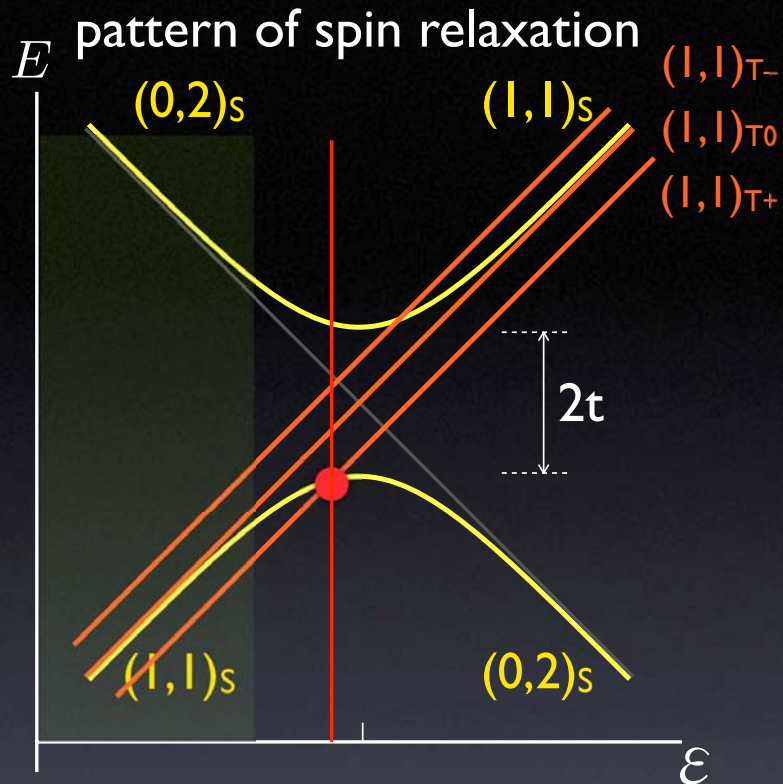


note:  
 $t$  is much larger than in relaxation experiment to allow rapid switching

# Measuring Spin Dephasing ( $T_2^*$ ): Time-domain Interferometry



dephasing causes failure  
to return to  $(0,2)$

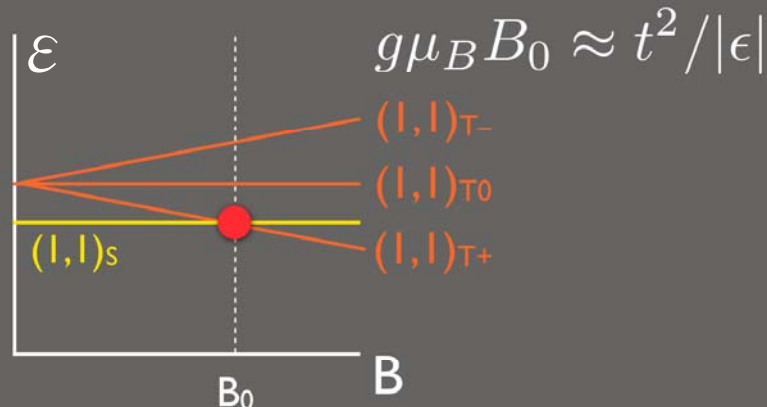


### ● S - $T_+$ degeneracy

$$E_{(1,1)_S} = E_{(1,1)_{T_+}} \text{ where}$$

$$E_{(1,1)_S} = -\sqrt{(\epsilon/2)^2 + t^2},$$

$$E_{(1,1)_{T_+}} = -\epsilon/2 - mg\mu_B B.$$

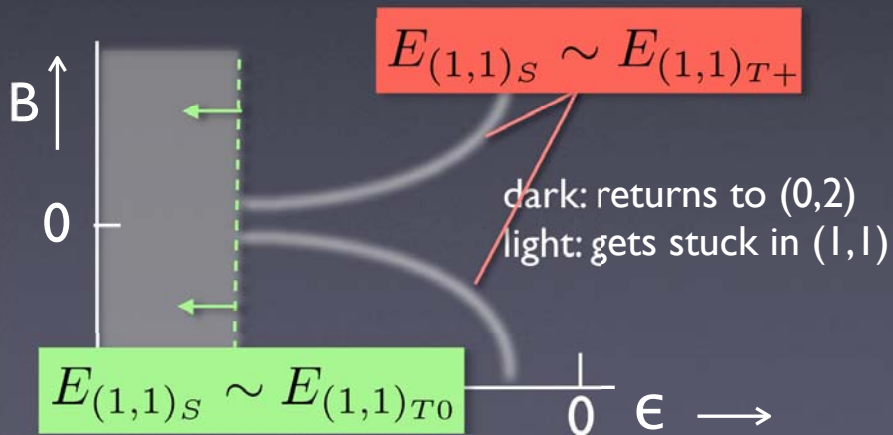


### ● S - $T_0$ degeneracy

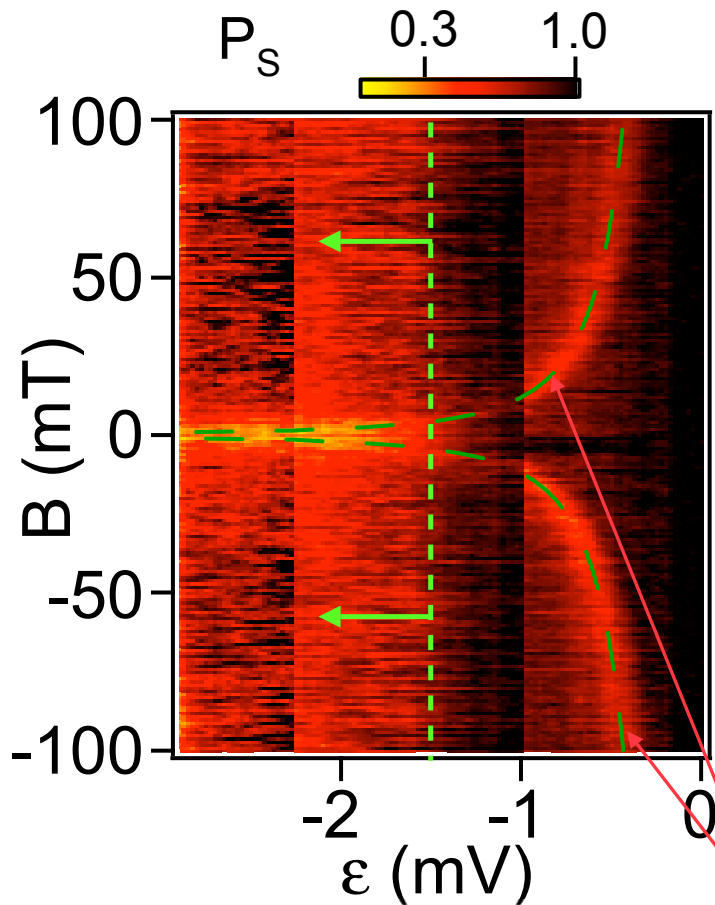
$$E_{(1,1)_S} \sim E_{(1,1)_{T_0}}$$

at large  $\epsilon$

so that  $t^2/|\epsilon| \approx g\mu_B B_{nuc}$ .

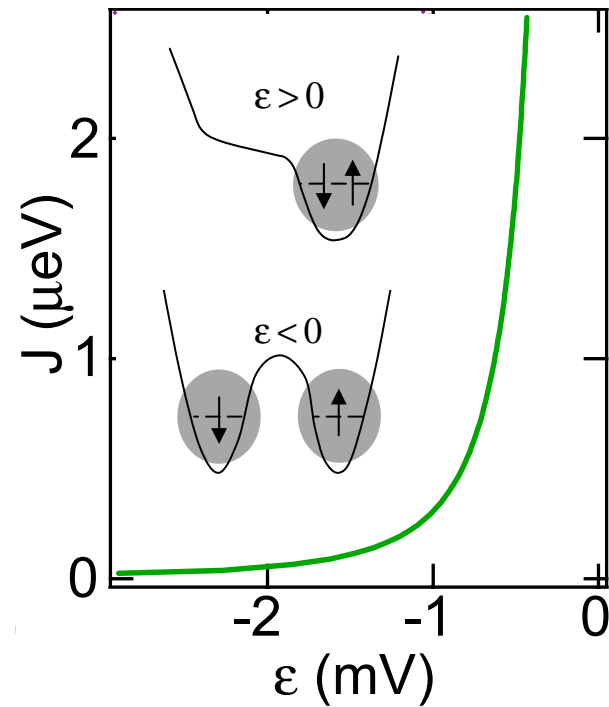


# Probability for separated singlet to be found in a singlet state after 200 ns.



S -  $T_+$  degeneracy occurs at

$$J(\epsilon) = g\mu_B B$$



$$E_{(1,1)_S} \sim E_{(1,1)_{T_0}}$$

$$E_{(1,1)_S} \sim E_{(1,1)_{T_+}}$$

# Determination of the Average Singlet-Triplet Splitting in Biradicals by Measurement of the Magnetic Field Dependence of CIDNP<sup>1</sup>

G. L. Closs,\* C. E. Doubleday

Department of Chemistry, The University of Chicago  
Chicago, Illinois 60637

Received January 27, 1973

5/eq 6; this equals  $k_2/(k_{-1} + k_2)$ . The proposed change in rate-determining step<sup>2</sup> requires that  $k_{-1} > k_2$ , so that Scheme I predicts an increased yield at lower pH. The results given in Table

Table I. Partitioning of a Formylphenylalanylthym Intermediate between Water and Formylhydrazine as a Function of pH<sup>a</sup>

pH	[Amine], <sup>b</sup> M	[Enzyme], M	% amid <sup>c</sup> formed <sup>d</sup>
7.5	0.0505	$1 \times 10^{-7}$	5.76
7.5	0.101	$1 \times 10^{-7}$	10.5
6.0	0.0505	$4 \times 10^{-6}$	5.56
6.0	0.101	$4 \times 10^{-6}$	10.7
4.5	0.0493	$1 \times 10^{-4}$	5.44
4.5	0.0986	$1 \times 10^{-4}$	10.2

<sup>a</sup> Reactions were run at 25° in 0.1 M KCl with an initial concentration of *N*-formyl-<sup>14</sup>C-phenylalanine methyl ester ( $2.18 \times 10^6$  cpm/ $\mu$ mol) of 0.7 mM. The pH was controlled with a pH stat and reactions were followed to completion as indicated by a cessation of proton release. <sup>b</sup> Concentration of the amine free base. <sup>c</sup> The yield of amide was determined by an isotope dilution technique. <sup>d</sup> Equal to (% amide)/(% carboxylic acid) (concentration of the amine free base).

consistent with Scheme I; acyl enzyme partitioning between water and formylhydrazine is invariant over the range pH 7.5–4.5. Scheme I does not apparently describe the enzyme-catalyzed hydrolysis of formylphenylalanine formylhydrazide.

Barry Zeeberg, Michael Caswell, Michael Caplow\*  
Department of Biochemistry, University of North Carolina  
Chapel Hill, North Carolina 27514  
Received November 22, 1972

## Determination of the Average Singlet-Triplet Splitting in Biradicals by Measurement of the Magnetic Field Dependence of CIDNP<sup>1</sup>

Sir:

We have previously reported the CIDNP spectra of alkenal products resulting from photochemical  $\alpha$  cleavage of alicyclic ketones.<sup>2</sup> We now report measure-

(1) Supported by grants from the Petroleum Research Fund (3965 C-4), administered by the American Chemical Society, and the National Science Foundation (GP 15719X).

(2) G. L. Closs and C. E. Doubleday, *J. Amer. Chem. Soc.*, **94**, 9248 (1972).

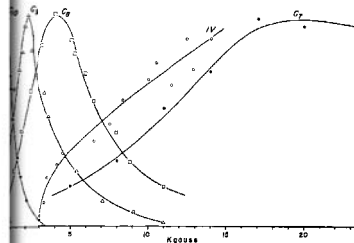
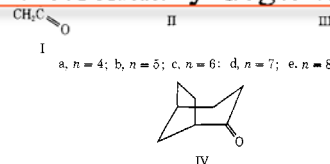


Fig. 1. Intensities of aldehyde proton emission signals of III-a (C<sub>1</sub>-C<sub>2</sub>) and of aldehyde derived from IV, as function of magnetic field. The intensities are in arbitrary units and not normalized among the different compounds.

Moreover, the principal hyperfine-induced singlet-triplet mixing will occur between the T<sub>-</sub> and S states.<sup>2</sup> By varying the magnetic field  $H_0$  in which the biradical is created, one can shift the T<sub>-</sub> level (with energy  $g\beta H_0$  below the T<sub>0</sub> level) to become essentially degenerate with the S level.

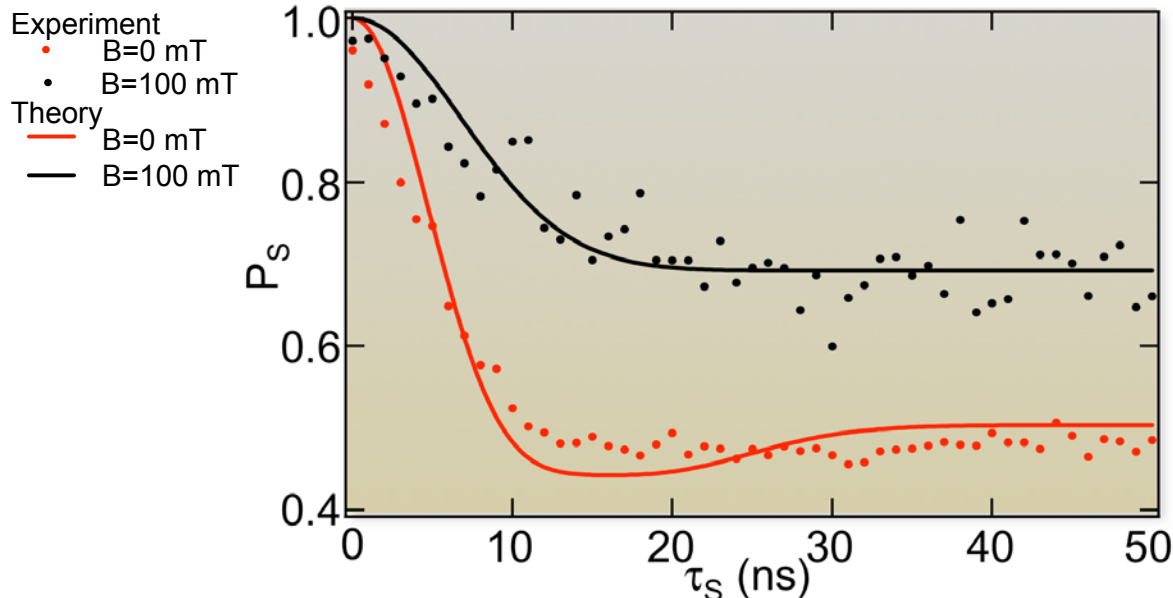
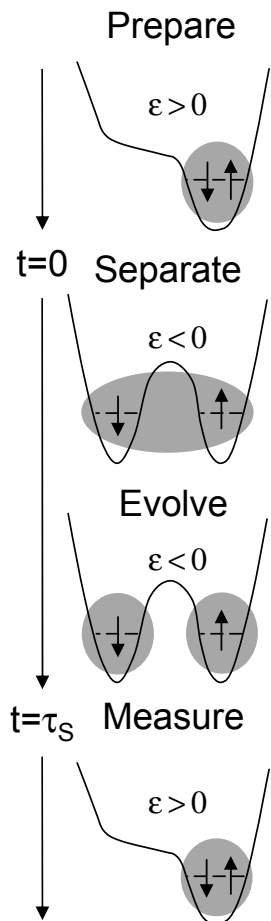


sample of ketone in chloroform placed between the pole pieces of a Varian 12-in. magnet at the desired field strength. The sample was then transferred quickly to the probe of an HA-100 spectrometer, and the aldehyde CIDNP signal was immediately recorded on a CAT. For each ketone, the relative integrated intensity of aldehyde CIDNP signal is plotted as a function at the field strength at which the sample was irradiated and is displayed in the curves of Figure 1.

These curves show two striking features. As the length of the biradical increases, the maxima move to lower energies, and the curve widths decrease dramatically. The first of these phenomena is straightforward to interpret.

For simplicity we first consider a fictitious, totally rigid biradical of the type II with a singlet-triplet splitting  $2J$ , corresponding to an effective exchange Hamiltonian  $-J(S_1 + 2S_2 \cdot S_3)$ . Moreover, the principal hyperfine-induced singlet-triplet mixing will occur between the T<sub>-</sub> and S states.<sup>2</sup> By varying the magnetic field  $H_0$  in which the biradical is created, one can shift the T<sub>-</sub> level (with energy  $g\beta H_0$  below the T<sub>0</sub> level) to become essentially degenerate with the S level. From

# Measuring Spin Dephasing ( $T_2^*$ )



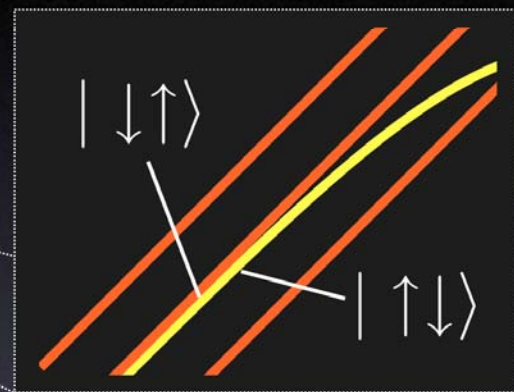
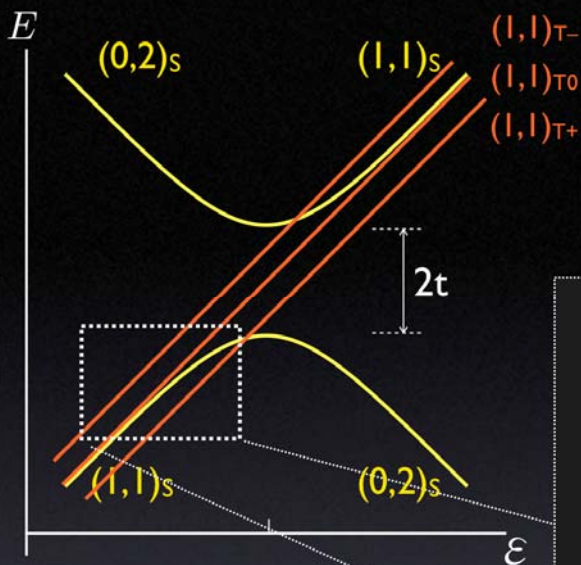
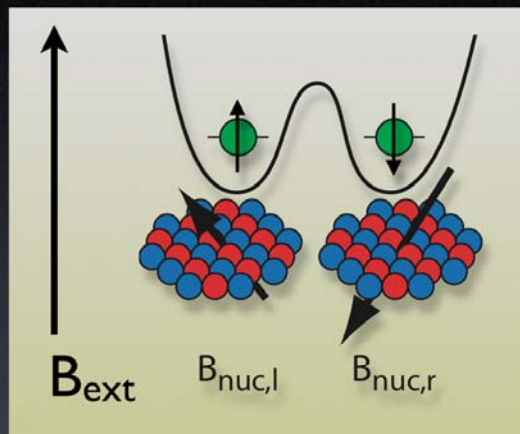
$$P_S(\tau_S) = 1 - \frac{C_1}{2} \left( 1 - e^{-(\tau_S/T_2^*)^2} \right) \text{ for } B \gg B_{\text{nuc}}$$

$$P_S(\tau_S) = 1 - \frac{3}{4} C_2 \left\{ 1 - \frac{1}{9} \left( 1 - 2e^{-\frac{1}{2}(\tau_S/T_2^*)^2} \left\{ (\tau_S/T_2^*)^2 - 1 \right\} \right)^2 \right\} \text{ for } B \ll B_{\text{nuc}}$$

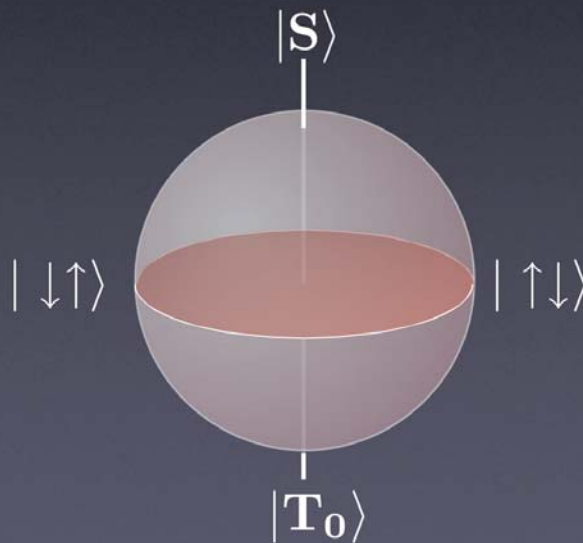
See: K. Schulten and P. G. Wolynes, *J. Chem. Phys.* **68** 3292 (1978); J. M. Taylor, *et al.* (in prep).

J. R. Petta, A. C. Johnson, J. Taylor, A. Yacoby, M. D. Lukin, M. Hanson, A. C. Gossard, *CMM, Science* (in press) (2005)

In the  $(1,1) S - T_0$  subspace, the eigenstates of the nuclear fields are  $|\uparrow\downarrow\rangle$  and  $|\downarrow\uparrow\rangle$ .



Bloch sphere in  $(1,1) S - T_0$  subspace



## Universal Quantum Computation with Spin-1/2 Pairs and Heisenberg Exchange

Jeremy Levy

Center for Oxide-Semiconductor Materials for Quantum Computation, and Department of Physics and Astronomy,  
University of Pittsburgh, 3941 O'Hara Street, Pittsburgh, Pennsylvania 15260

(Received 23 January 2001; published 17 September 2002)

An efficient and intuitive framework for universal quantum computation is presented that uses pairs of spin-1/2 particles to form logical qubits and a single physical interaction, Heisenberg exchange, to produce all gate operations. Only two Heisenberg gate operations are required to produce a controlled  $\pi$ -phase shift, compared to nineteen for exchange-only proposals employing three spins. Evolved from well-studied decoherence-free subspaces, this architecture inherits immunity from collective decoherence mechanisms. The simplicity and adaptability of this approach should make it attractive for spin-based quantum computing architectures.

DOI: 10.1103/PhysRevLett.89.147902

PACS numbers: 03.67.Lx, 75.10.Jm, 89.70.+c

Quantum computation involves the initialization, controlled evolution, and measurement of a quantum system consisting of  $n$  two-level quantum subsystems known

$\exp[-i\theta\hat{H}_{ij}^\alpha/gB^\alpha]$ . These physical qugates are combined to create logical qugates that are known to be universal [3]. The choice of physical qugate sets is not

An efficient and intuitive framework for universal quantum computation is presented that uses pairs of spin-1/2 particles to form logical qubits and a single physical interaction, Heisenberg exchange, to produce all gate operations.

ary set of logical qubits and qugates that are known to generate all possible unitary operations [3]. The logical qubits and qugates are then "simulated" by physical qubits and qugates.

It is highly desirable from an experimentalist's perspective to use the smallest possible set of physical qugates, since each brings its own complexities and difficulties. The Heisenberg exchange ( $\hat{H}_{ij} = J\hat{S}_i \cdot \hat{S}_j$ ) and Zeeman magnetic ( $\hat{H}_i^\alpha = g\hat{S}_i^\alpha B^\alpha$ ) interactions figure prominently in proposals that employ electron [4–6] or nuclear [7] spin physical qubits. (Spins are indexed by subscripts, Cartesian coordinates are indexed by superscripts,  $\hat{S}_i^\alpha$  are spin-1/2 operators that satisfy  $[\hat{S}_i^\alpha, \hat{S}_i^\beta] = i\epsilon^{\alpha\beta\gamma}\hat{S}_i^\gamma$ , and  $\hbar = \mu_B = 1$ .) Using a terminology appropriate for electron spin, universal quantum computation requires temporal control over a minimum of  $n - 1$  two-body exchange operators and two one-body magnetic operators. Experimentally, these physical qugates are modulated via coupling constants that are controlled by classical (e.g., electric or magnetic) fields. For electron spins, the exchange strength  $J$  is controlled by the electron charge, which is in turn controlled by applied electric fields [4,7]; the Landé  $g$  factor can be controlled by the choice of surrounding medium [4], and a variety of magnetic inductions  $B^\alpha$  are available. The Heisenberg exchange and Zeeman rotation coupling constants are modulated in time to produce corresponding unitary operators  $\hat{e}_{ij}(\theta) = \exp[-i\theta\hat{H}_{ij}/J]$  and  $\hat{r}_i^\alpha(\theta) =$

Recently, there has been a great deal of theoretical activity involving decoherence-free subspaces [8] (DFS). In this framework, qubits are identified with particular subspaces of  $c$  physical qubits that commute with a particular symmetry of the time-independent full Hamiltonian (e.g., rotational symmetry) [9]. The consequences of this requirement are striking: in forming qubits from a two-dimensional subspace of  $c$  spin-1/2 particles with a definite total  $z$  component  $m$  [known as DFS,  $(m)$ ], exchange interactions formed into magnetic interactions *becomes universal*. One consequence is that the exchange interactions would process, but for  $c > 2$  there are universal quantum computation. I found 19 to be the minimum number of physical qubits required to implement cNOT with  $c = 3$ , and [10]. Logical qubit rotations generated by four physical qugate operations, dependent on the strength of coupling within the qubit.

One might wonder why logical spin-1/2 pairs are not used. The qubit is DFS<sub>2</sub>(0), spanned by  $|10\rangle_c$ . Heisenberg exchange between two qubits produces rotations about axis [11]:  $\hat{H}_{12} = (|01\rangle\langle 10|_c + |10\rangle\langle 01|_c)/2 = \hat{S}_1^x \hat{S}_2^x$  generates un-

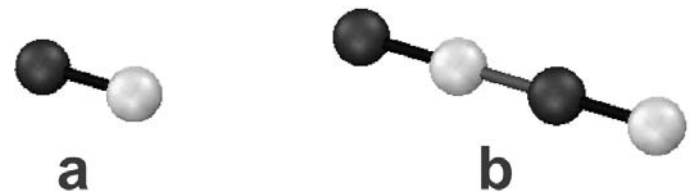
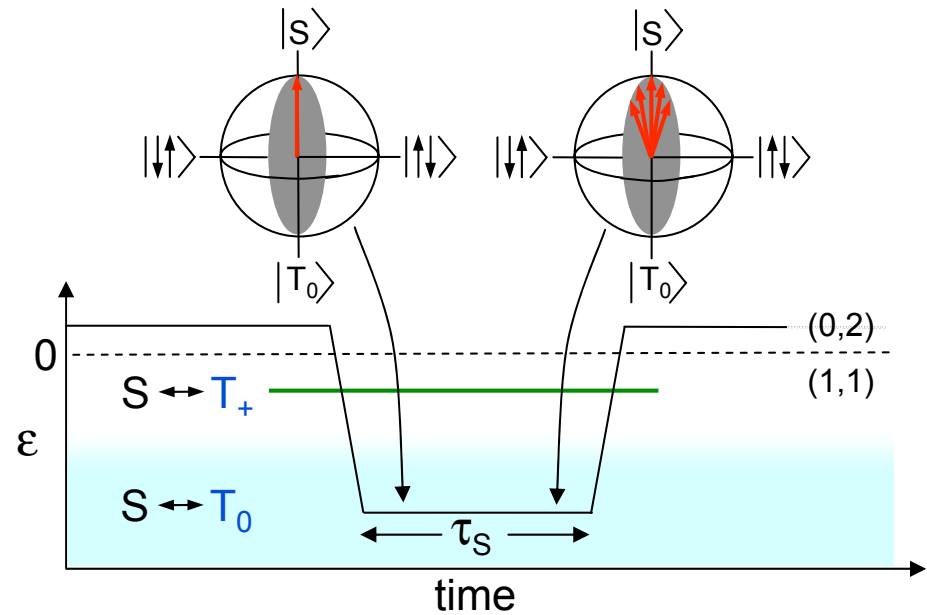
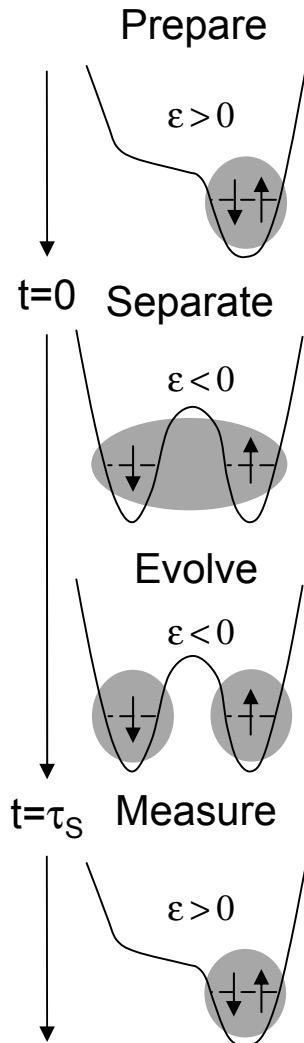
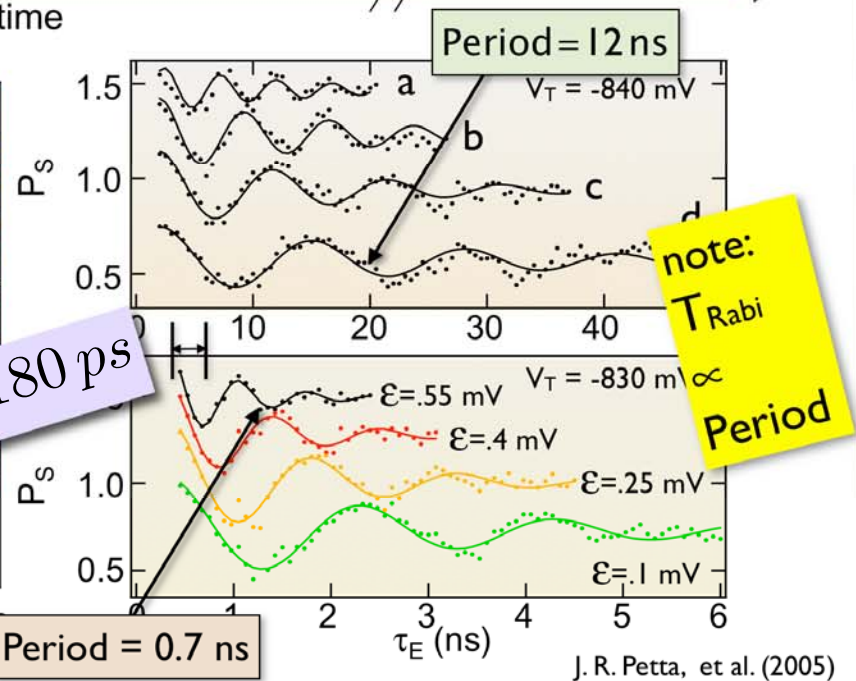
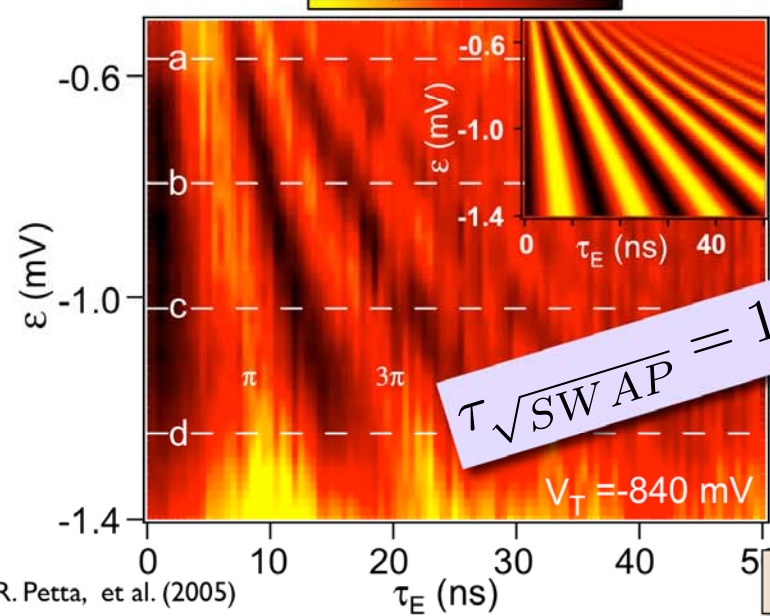
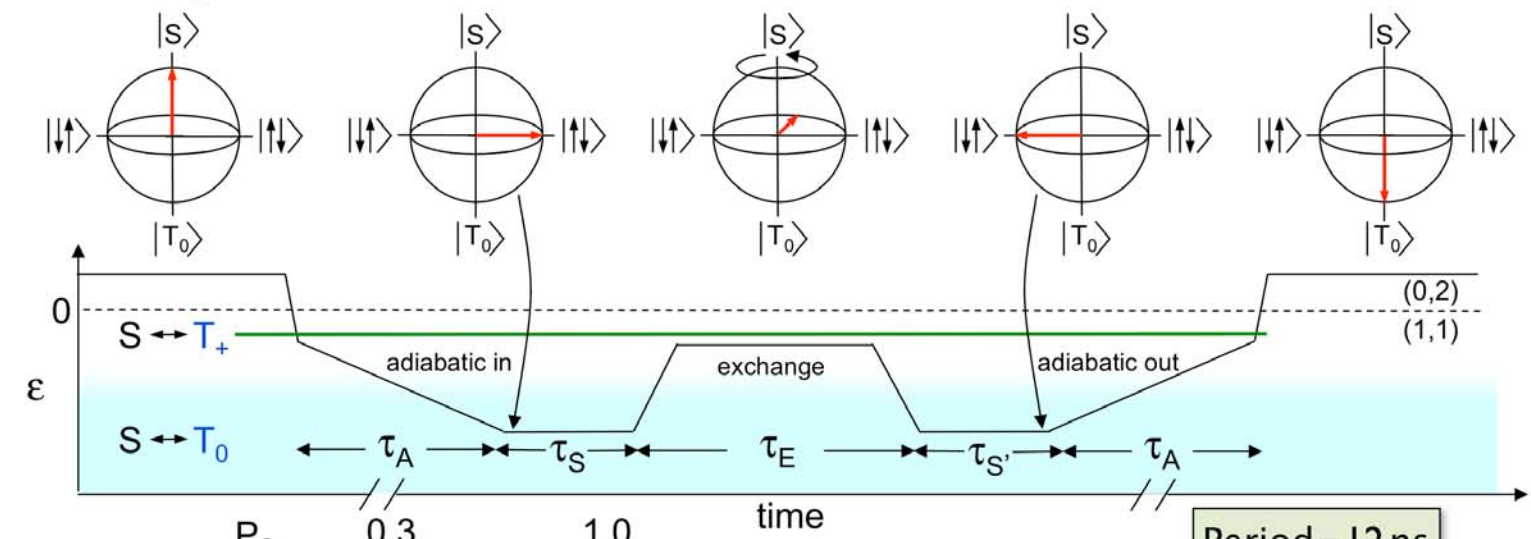


FIG. 1. (a) Logical qubit  $Q$  formed from the  $S_z = 0$  subspace of two spin-1/2 physical qubits with different Landé  $g$  factors  $g_1$  (gray) and  $g_2$  (white). Heisenberg coupling within the logical qubit is represented by a solid black line. (b) Two logical qubits coupled via Heisenberg exchange, represented by a solid gray line.

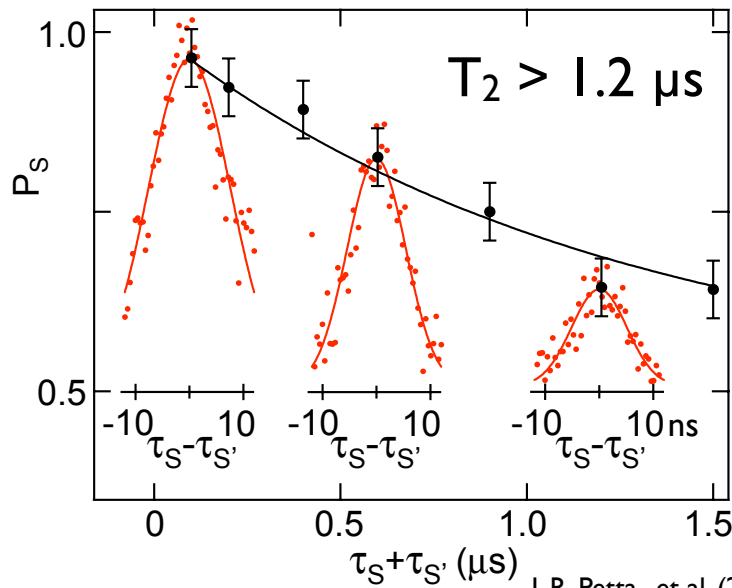
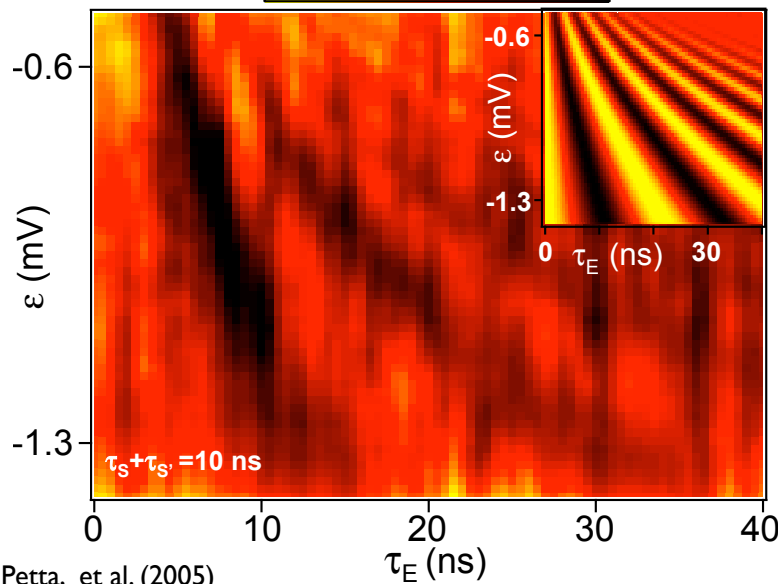
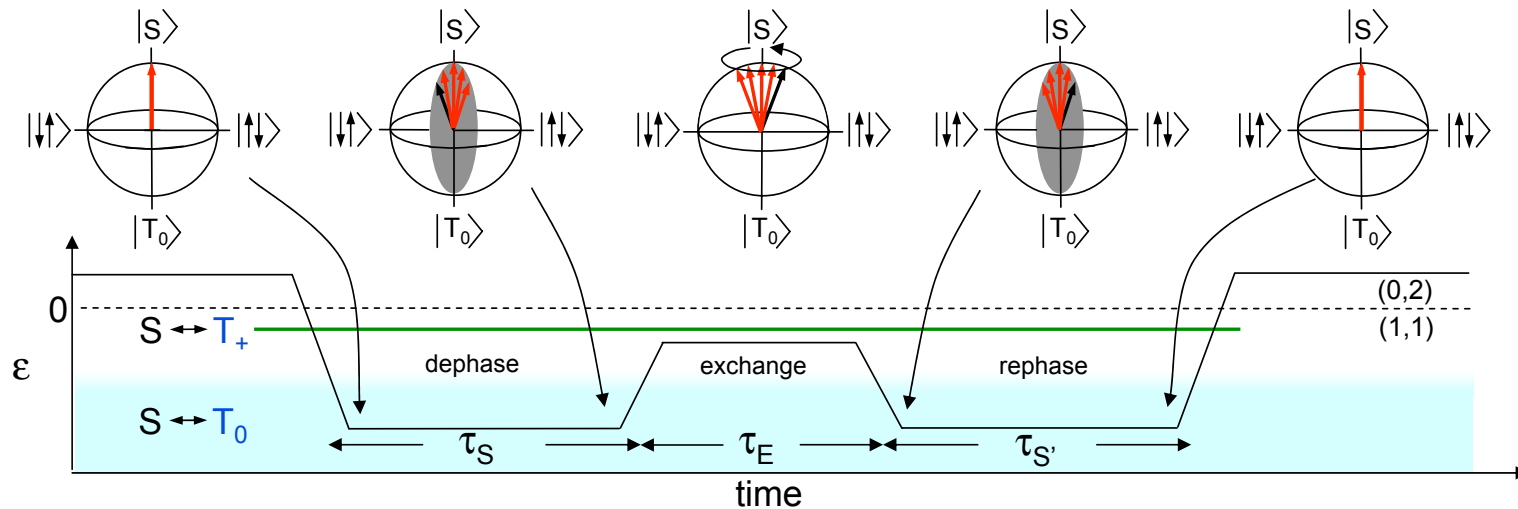
# Probability for separated singlet to be found in a singlet after time $\tau_S$



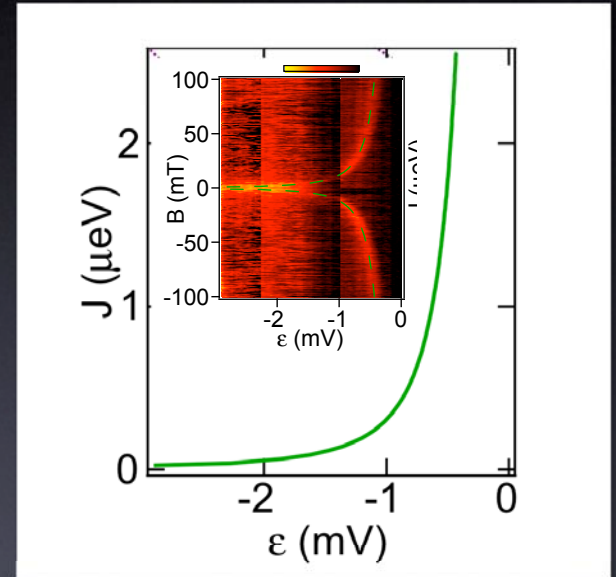
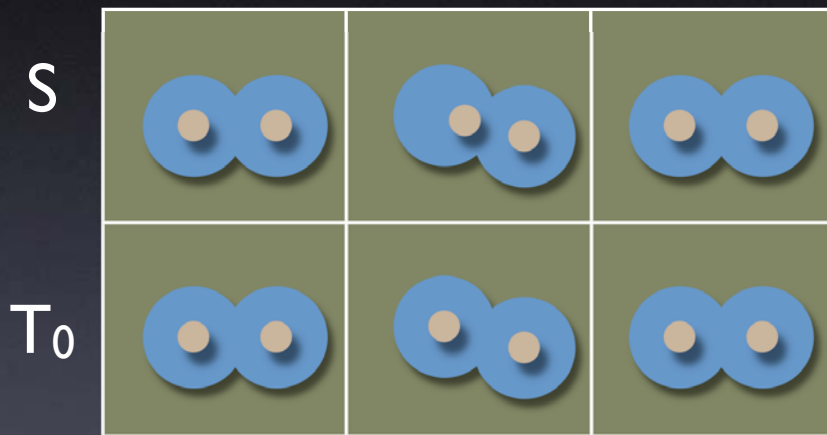
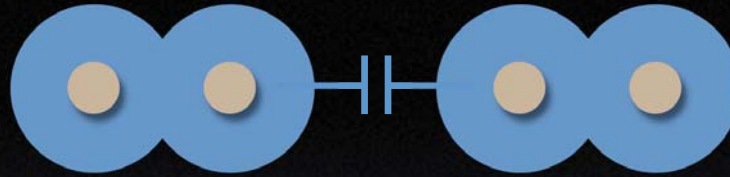
# Exchange Control: Rabi oscillations between $\uparrow\downarrow$ and $\downarrow\uparrow$ states



# Spin Echo in S - T<sub>0</sub> basis



# Electrostatic Two-Qubit Gate



$$\frac{dJ}{d\epsilon} \sim 0 \quad \frac{dJ}{d\epsilon} \sim \frac{\pi d}{e\tau} \quad \frac{dJ}{d\epsilon} \sim 0$$

# Determination of the Average Singlet-Triplet Splitting in Biradicals by Measurement of the Magnetic Field Dependence of CIDNP<sup>1</sup>

G. L. Closs,\* C. E. Doubleday

Department of Chemistry, The University of Chicago  
Chicago, Illinois 60637

Received January 27, 1973

5/eq 6; this equals  $k_2/(k_{-1} + k_2)$ . The proposed change in rate-determining step<sup>2</sup> requires that  $k_{-1} > k_2$ , so that Scheme I predicts an increased yield at lower pH. The results given in Table

Table I. Partitioning of a Formylphenylalanylthym Intermediate between Water and Formylhydrazine as a Function of pH<sup>a</sup>

pH	[Amine], <sup>b</sup> M	[Enzyme], M	% amide formed <sup>c</sup>
7.5	0.0505	$1 \times 10^{-7}$	5.76
7.5	0.101	$1 \times 10^{-7}$	10.5
6.0	0.0505	$4 \times 10^{-6}$	5.56
6.0	0.101	$4 \times 10^{-6}$	10.7
4.5	0.0493	$1 \times 10^{-4}$	5.44
4.5	0.0986	$1 \times 10^{-4}$	10.2

<sup>a</sup> Reactions were run at 25° in 0.1 M KCl with an initial concentration of *N*-formyl-<sup>14</sup>C-phenylalanine methyl ester ( $2.18 \times 10^6$  cpm/ $\mu$ mol) of 0.7 mM. The pH was controlled with a pH stat and reactions were followed to completion as indicated by a cessation of proton release. <sup>b</sup> Concentration of the amine free base. <sup>c</sup> The yield of amide was determined by an isotope dilution technique. <sup>d</sup> Equal to (% amide)/(% carboxylic acid) (concentration of the amine free base).

consistent with Scheme I; acyl enzyme partitioning between water and formylhydrazine is invariant over the range pH 7.5–4.5. Scheme I does not apparently describe the enzyme-catalyzed hydrolysis of formylphenylalanine formylhydrazide.

Barry Zeeberg, Michael Caswell, Michael Caplow\*  
Department of Biochemistry, University of North Carolina  
Chapel Hill, North Carolina 27514  
Received November 22, 1972

## Determination of the Average Singlet-Triplet Splitting in Biradicals by Measurement of the Magnetic Field Dependence of CIDNP<sup>1</sup>

Sir:

We have previously reported the CIDNP spectra of alkenal products resulting from photochemical  $\alpha$  cleavage of alicyclic ketones.<sup>2</sup> We now report measure-

(1) Supported by grants from the Petroleum Research Fund (3965 C-4), administered by the American Chemical Society, and the National Science Foundation (GP 15719X).

(2) G. L. Closs and C. E. Doubleday, *J. Amer. Chem. Soc.*, **94**, 9248 (1972).

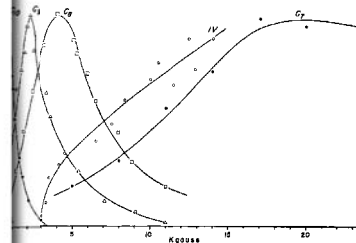
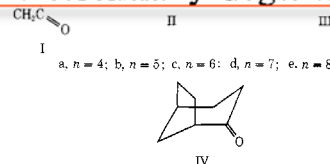


Fig. 1. Intensities of aldehyde proton emission signals of III-a (C<sub>1</sub>-C<sub>2</sub>) and of aldehyde derived from IV, as function of magnetic field. The intensities are in arbitrary units and not normalized among the different compounds.

Moreover, the principal hyperfine-induced singlet-triplet mixing will occur between the T<sub>-</sub> and S states.<sup>2</sup> By varying the magnetic field  $H_0$  in which the biradical is created, one can shift the T<sub>-</sub> level (with energy  $g\beta H_0$  below the T<sub>0</sub> level) to become essentially degenerate with the S level.



sample of ketone in chloroform placed between the pole pieces of a Varian 12-in. magnet at the desired field strength. The sample was then transferred quickly to the probe of an HA-100 spectrometer, and the aldehyde CIDNP signal was immediately recorded on a CAT. For each ketone, the relative integrated intensity of aldehyde CIDNP signal is plotted as a function at the field strength at which the sample was irradiated and is displayed in the curves of Figure 1.

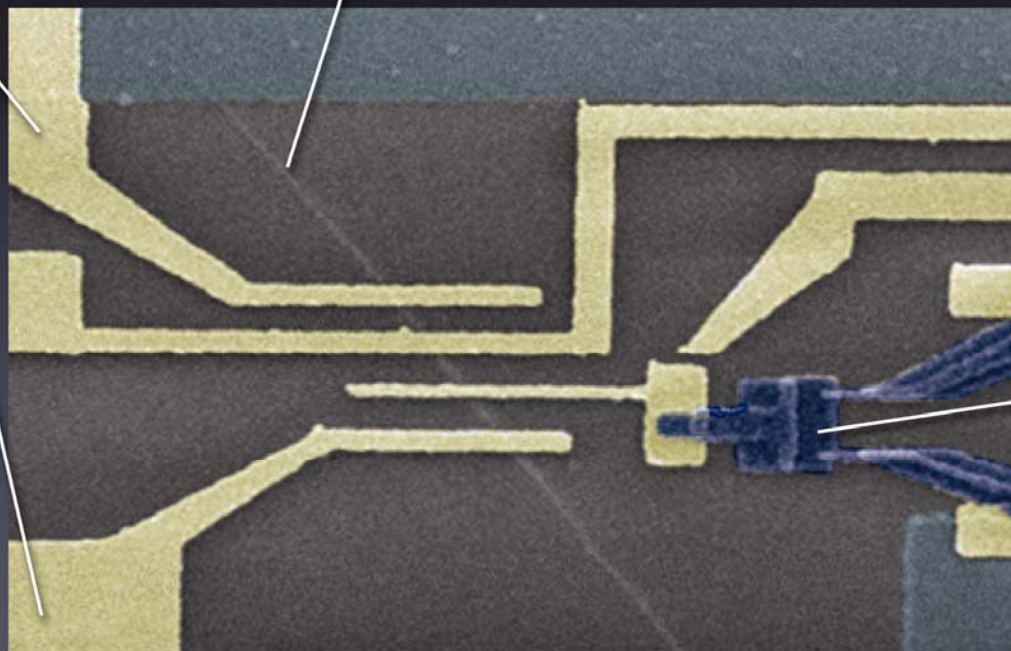
These curves show two striking features. As the length of the biradical increases, the maxima move to lower energies, and the curve widths decrease dramatically. The first of these phenomena is straightforward to interpret.

For simplicity we first consider a fictitious, totally rigid biradical of the type II with a singlet-triplet splitting  $2J$ , corresponding to an effective exchange Hamiltonian  $-J(S_1 + 2S_2 \cdot S_3)$ . Moreover, the principal hyperfine-induced singlet-triplet mixing will occur between the T<sub>-</sub> and S states.<sup>2</sup> By varying the magnetic field  $H_0$  in which the biradical is created, one can shift the T<sub>-</sub> level (with energy  $g\beta H_0$  below the T<sub>0</sub> level) to become essentially degenerate with the S level. From

# Nanotube-Based Single Electron Device with Fast Charge Sensor

depletion  
gates

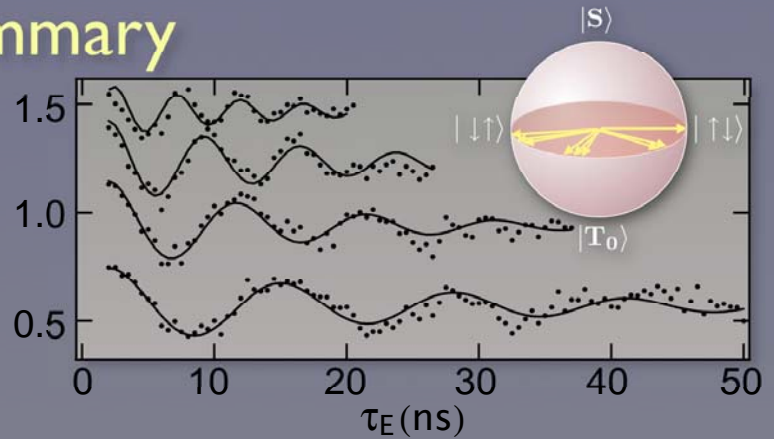
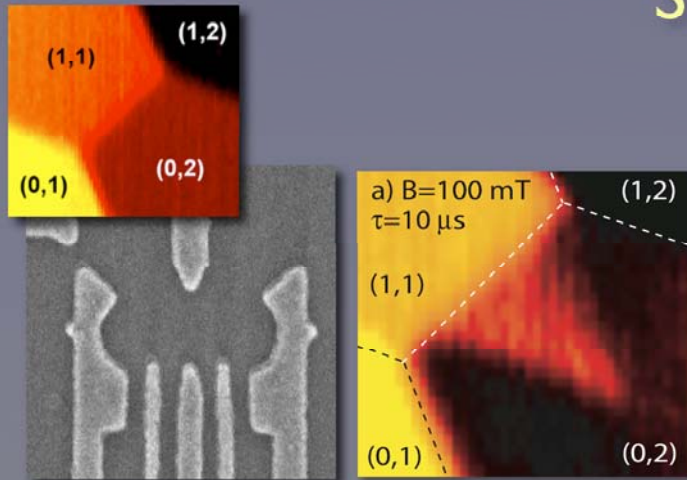
carbon nanotube



rf SET

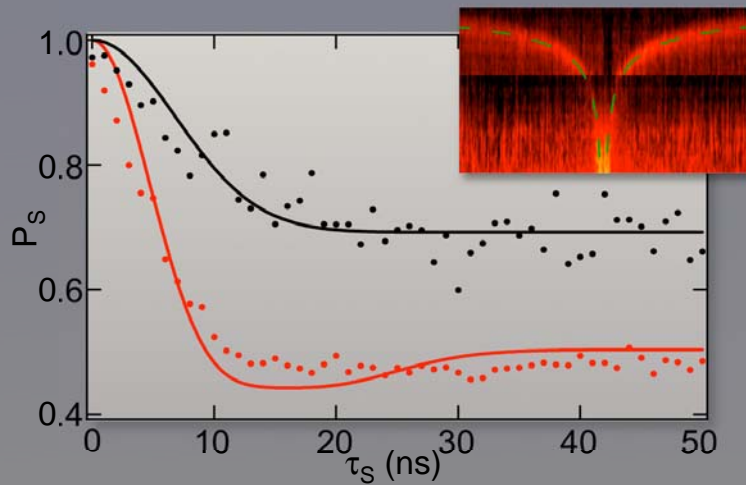
M. J. Biercuk, et al. [in collaboration with R. Clark, UNSW] (in preparation).

# Summary

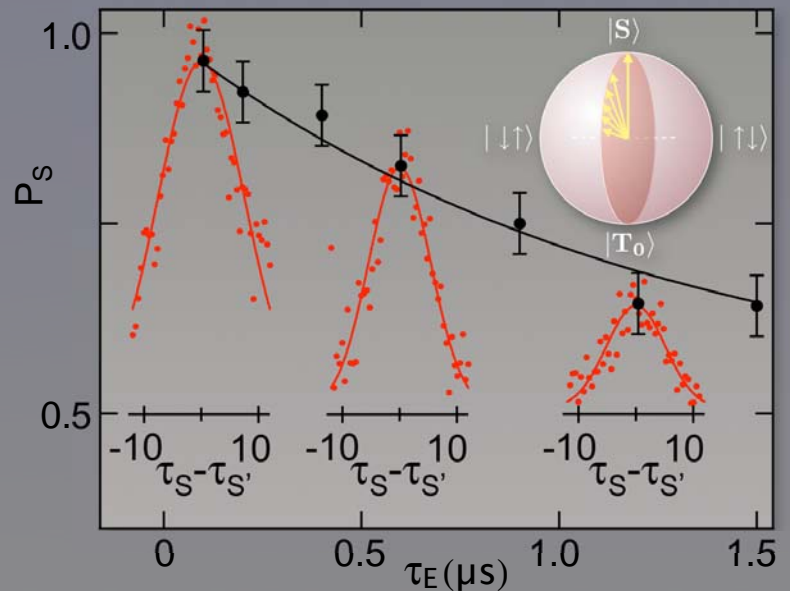


## Spin Rabi and swap operations

Spin  $T_1 \sim 1-10$ ms



Spin  $T_2^* \sim 10$ ns



Spin Echo - Spin  $T_2 > 1$   $\mu$ s